Integral techno-economic comparison and greenhouse gas balances of different production routes of aromatics from biomass with CO2 capture

Yang, Fan; Meerman, Hans; Zhang, Zhenhua; Jiang, Jianrong; Faaij, André

Published in:
Journal of Cleaner Production

DOI:
10.1016/j.jclepro.2022.133727

Publication date:
2022

Journal of Cleaner Production 372 (2022) 133727

Contents lists available at ScienceDirect

Journal of Cleaner Production

journal homepage: www.elsevier.com/locate/jclepro

Integral techno-economic comparison and greenhouse gas balances of different production routes of aromatics from biomass with CO_2 capture

Fan Yang [a,*], Hans Meerman [a], Zhenhua Zhang [b,c], Jianrong Jiang [d], André Faaij [a,e]

[a] Integrated Research on Energy, Environment and Society, University of Groningen, Nijenborgh 6, 9747, AG, Groningen, the Netherlands
[b] Genomics Coordination Center, University of Groningen and University Medical Center Groningen, Antonius Deusinglaan 1, 9713, AV, Groningen, the Netherlands
[c] Department of Genetics, University of Groningen and University Medical Center Groningen, Antonius Deusinglaan 1, 9713, AV, Groningen, the Netherlands
[d] Shaanxi Key Laboratory of Energy Chemical Process Intensification, School of Chemical Engineering and Technology, Xi'an Jiaotong University, Xi'an, Shaanxi, 710049, China
[e] TNO Energy Transition, Princetonlaan 6, 3584, CB, Utrecht, the Netherlands

ARTICLE INFO

Handling editor: Pai Zheng

Keywords:
Aromatics
Greenhouse gas reduction
Biomass
Biomass combined with CO_2 capture and storage
CO_2 avoidance cost

ABSTRACT

The techno-economic performance and CO_2 equivalent (CO_{2eq}) reduction potential of bio-based aromatic production cases with and without CO_2 capture and storage (CCS) have been evaluated and compared to those of fossil-based aromatic production. The bio-cases include tail gas reactive pyrolysis (TGRP), catalytic pyrolysis (CP), hydrothermal liquefaction (HTL), gasification-methanol-aromatics (GMA), and Diels-Alder of furan/furfural combined with catalytic pyrolysis of lignin (FFCA). The crude oil-based naphtha catalytic reforming (NACR) routes have GHG emissions of 43.4 and 43.9 t CO_{2eq}/t aromatics with and without CCS (NACR-CCS), respectively. Except for HTL, all the biomass cases with CCS show negative emissions between −6.1 and −1.1 t CO_{2eq}/t aromatics with avoidance costs ranging from 27.7 to 93.3 $/t CO_{2eq}. Under favorable conditions, GMA with CCS (GMA-CCS) has the lowest emissions (−14.6 t CO_{2eq}/t aromatics), while CP with CCS (CP-CCS) shows the lowest avoidance cost (12.3 $/t CO_{2eq}). All biomass based aromatics production techniques are currently at the laboratory or demonstration stages, except for CP, which has pilot plants. The results indicate that bio-based aromatics production, with their reasonable avoidance costs and low, or potentially negative, greenhouse gas (GHG) emissions, are an attractive option to compensate for the expected aromatic production shortages in the coming decades.

1. Introduction

Globally, the petro-chemical industry is the largest industrial energy consumer and the third largest industrial subsector of direct greenhouse gas (GHG) emissions in the world (IEA, 2021, 2017a; Yang et al., 2021b). Additionally, the petro-chemical industry is expected to account for approximately 33% and 50% of the global crude oil demand by 2030 and 2050, respectively (OECD/IEA, 2018a). One reason for this increase is the expected reduction in the demand for gasoline and diesel due to the rise of alternative transportation fuels, such as electricity and hydrogen (AFC TCP, 2018; BP, 2020; IEA, 2019a, 2017b). Global aromatics production is also expected to grow from 107.5 Mt in 2017 to 144.5 Mt in 2030 and 160 Mt in 2035 as they make up 40% of plastics' composition (OECD/IEA, 2018b). Almost all (97%) aromatics are currently produced as by-products after refining crude oil into transportation fuels; the remaining 3% of aromatics come from coal-based coke oven oil (Bender, 2013). In the future, the decrease in the demand for petroleum transport fuel would decrease the associated aromatic production. As the demand for aromatics is expected to increase, this combination could result in a shortage of aromatics. Additionally, the fossil CO_2 emissions during the use and disposal phases are nearly impossible to capture due to the decentralized nature of these phases (He et al., 2021; Lok et al., 2019). To combat climate change and the expected production shortages, sustainable bio-based production methods have emerged (Anellotech, 2019; Lok et al., 2019; Miandad et al., 2019).

Aromatics can be produced from various biomass sources (Fig. 1) including raw biomass, such as animal manure (Sorunmu et al., 2017), algal biomass (Duan and Savage, 2011; Ross et al., 2010), lignocellulosic biomass (De Wild et al., 2014; McVey et al., 2020; Nanda et al., 2020), and the individual components of biomass, such as cellulose (Chen et al.,

Abbreviations: WGS, Water gas shift; AGR, Acid gas removal; PEF, Polyethylene furanoate; FEE, Furfuryl ethyl ether.

* Corresponding author.
E-mail address: F.Yang@rug.nl (F. Yang).

https://doi.org/10.1016/j.jclepro.2022.133727
Received 24 March 2022; Received in revised form 26 July 2022; Accepted 18 August 2022
Available online 28 August 2022

Abbreviations

ASU	Air separation unit
BECCS	Biomass combined with CO_2 capture and storage
BTX	Benzene, toluene and xylene
CCS	CO_2 capture and storage
CHP	Combined heat and power
CP	Catalytic pyrolysis
DMF	Dimethylformamide
DSTL	Distillation
FFCA	Diels-Alder of furan/furfur combined with catalytic pyrolysis of lignin
GHG	Greenhouse gas
GMA	Gasification-methanol-aromatics
GTM	Gasification to methanol
HTL	Hydrothermal liquefaction
LCB	Lignocellulosic biomass
LPG	liquefied petroleum gas
MDEA	Methyl diethanolamine
MTA	Methanol to aromatics
NACR	Naphtha catalytic reforming
NCG	Non-condensable gas
NG	Natural gas
NPV	Net present value
TCR	Total capital requirement
TGRP	Tail gas reactive pyrolysis
TIC	Total installed costs
TPC	Total plant cost
T&S	Transport and storage

2018), hemicellulose (Yang et al., 2019a), lignin (Yang et al., 2019c), and glucose (Foster et al., 2012). Vegetable and animal oils, such as peanut oil (Mo et al., 2017), rapeseed oil (Bielansky et al., 2011), palm oil (Bielansky et al., 2011), soybean oil (Bielansky et al., 2011; Zheng et al., 2019), and oleic acid (Dupain et al., 2007; He et al., 2021), are also being investigated. Lastly, certain bio-based products have significant aromatic-conversion potentials, for example, bio-methanol (Ji et al., 2018), bio-ethanol (Li et al., 2017b), fast pyrolysis (FP) oil (Vispute et al., 2010), furanics (Cheng and Huber, 2012), and certain bio-based industrial wastes, such as black liquor from pulp and paper mills (Heeres et al., 2018) and glycerol from biodiesel refinery plants (He et al., 2018; Nanda et al., 2020).

This study focuses on lignocellulosic biomass due to its high global abundance, and the technological reliability and data availability of the biomass conversion processes (Chen et al., 2019; Elkasabi et al., 2014; Hu et al., 2011; Zheng et al., 2017). The conversion routes investigated in this study are three thermochemical conversion methods, namely, pyrolysis (Ghorbannezhad et al., 2018; He et al., 2018; Zheng et al., 2014) including gas reactive pyrolysis (TGRP) and catalytic pyrolysis (CP), hydrothermal liquefaction (HTL) (Gerssen-Gondelach et al., 2014; Jensen et al., 2017), gasification-methanol-aromatics (GMA) (Jiang et al., 2020), and one biochemical conversion method, Diels–Alder reaction (Cheng and Huber, 2012; Wijaya et al., 2016).

The biomass based processes do not use fossil fuel as raw material, however, the GHG emissions of the entire lifecycle are still positive because the biomass production, harvest, and collection processes still emit fossil-based GHG emissions. Introducing CO_2 capture and storage (CCS) to the bio-aromatic routes results in an increasing carbon reduction potential as the biogenic CO_2 from the reaction processes and the CO_2 from onsite boilers can be captured. However, these bio-CCS (BECCS) options have received limited attention.

Several studies have investigated the techno-economic performance of bio-based aromatics. The production costs of pyrolysis routes have been estimated by (Lin et al., 2014) and (Athaley et al., 2019). These studies have analyzed the production cost of p-xylene from starch via CP and from lignocellulosic biomass via catalytic hydrolysis. The net present value (NPV) of methanol based BTX[1] has been investigated by (Jiang et al., 2020) and (Zhang et al., 2021a). (Vural Gursel et al., 2019) and (Corredor et al., 2019) investigated the NPV of bio-based aromatics from lignin and that of benzene converted from methane. For the aromatics produced from bio-based furans (Eerhart et al., 2014), evaluated the production costs of polyethylene furanoate (PEF) and furfuryl ethyl ether (FEE), which included the biomass-to-furans conversion processes but not the furans-to-aromatics conversion processes. These studies have reported a wide range of production costs from 1480 to 4121 $/t aromatics.

The technical performance of the studies mentioned above are difficult to compare with each other due to differences in feedstock input and design choices in the production processes. The economics have only been investigated for the pyrolysis processes, a part of the GMA process, and for conversion of furan to aromatics. Upstream and downstream GHG emissions are often not included, and CCS has not been applied to any of the production routes.

Therefore, this study investigated the techno-economic performance and cradle-to-grave GHG emissions of conventional and novel lignocellulosic-based aromatic production, with and without CCS. Five bio-based routes (TGRP, CP, HTL, GMA, and Diels–Alder reaction) were investigated via a harmonized methodology for assessing their process design, mass and energy yields, GHG emissions, and avoidance costs. This harmonized methodology enabled comparisons of different bio-based routes with each other and with the current petro-based route.

The rest of this paper is structured as follows. Section 2 introduces the methodology, system boundary, and the standardization of key parameters and data. Section 3 describes the detailed processes of different aromatics production routes including conventional technology and GHG mitigation technologies. Section 4 gives the techno-economic performance of the investigated routes and compares them with each other. Section 5 and 6 give the discussion and conclusions, respectively.

2. Methodology

2.1. System boundary

This study focuses on the conversion routes. The system boundaries used are shown in Fig. 2. A cradle-to-grave approach was used for the life cycle GHG assessments and a gate-to-gate approach was used for the techno-economic analyses. Results are expressed per 1 t aromatic production. Upstream emissions from biomass and fossil stock were included, but upstream emissions from the consumables (such as catalysts and CO_2 absorption solvents) were not. All the carbon from the flue gas and non-condensable gas (NCG), biochar, and unreacted biomass was assumed to generate CO_2, which is subsequently emitted to the atmosphere, and the biomass was set to be carbon neutral. A captive power plant utilizes the refinery bioenergy, such as NCGs, biochar, and unreacted biomass to produce steam (with efficiency of 80%) or electricity (with efficiency of 32%) (Eerhart et al., 2014; Hu et al., 2011; Scown et al., 2014). The bioenergy was first used to meet the internal demand of steam, and any excess bioenergy was used for electricity generation. If steam generation was insufficient to meet the internal demand, natural gas was imported. Electricity excess or shortage was

[1] BTX stands for benzene, toluene and xylene. They are the most basic aromatics.

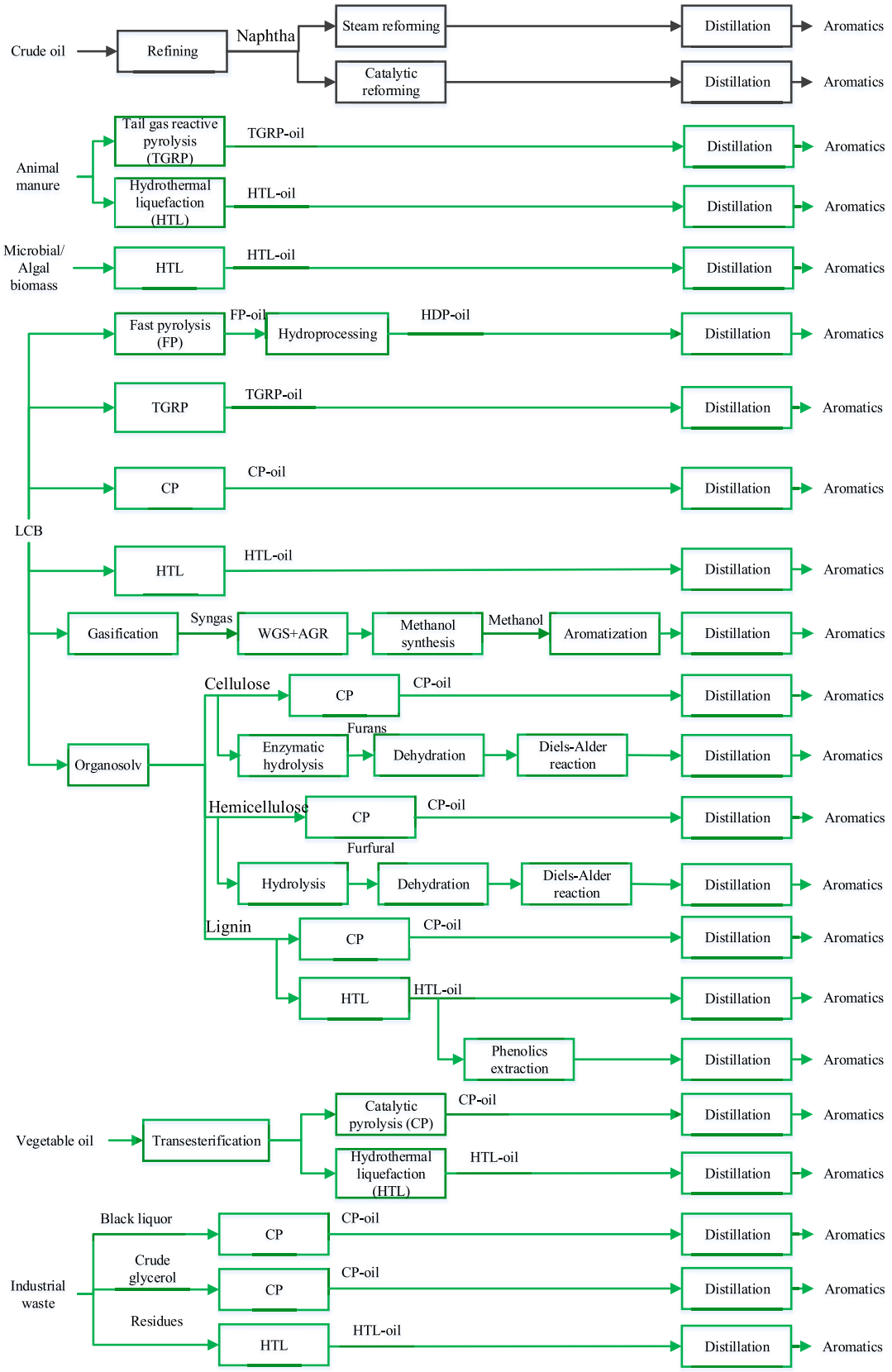

Fig. 1. Aromatics production from fossil and biomass sources with different technologies; the dark grey arrows and the green arrows represent the fossil based and bio-based aromatics production routes, respectively. (LCB = Lignocellulosic biomass).

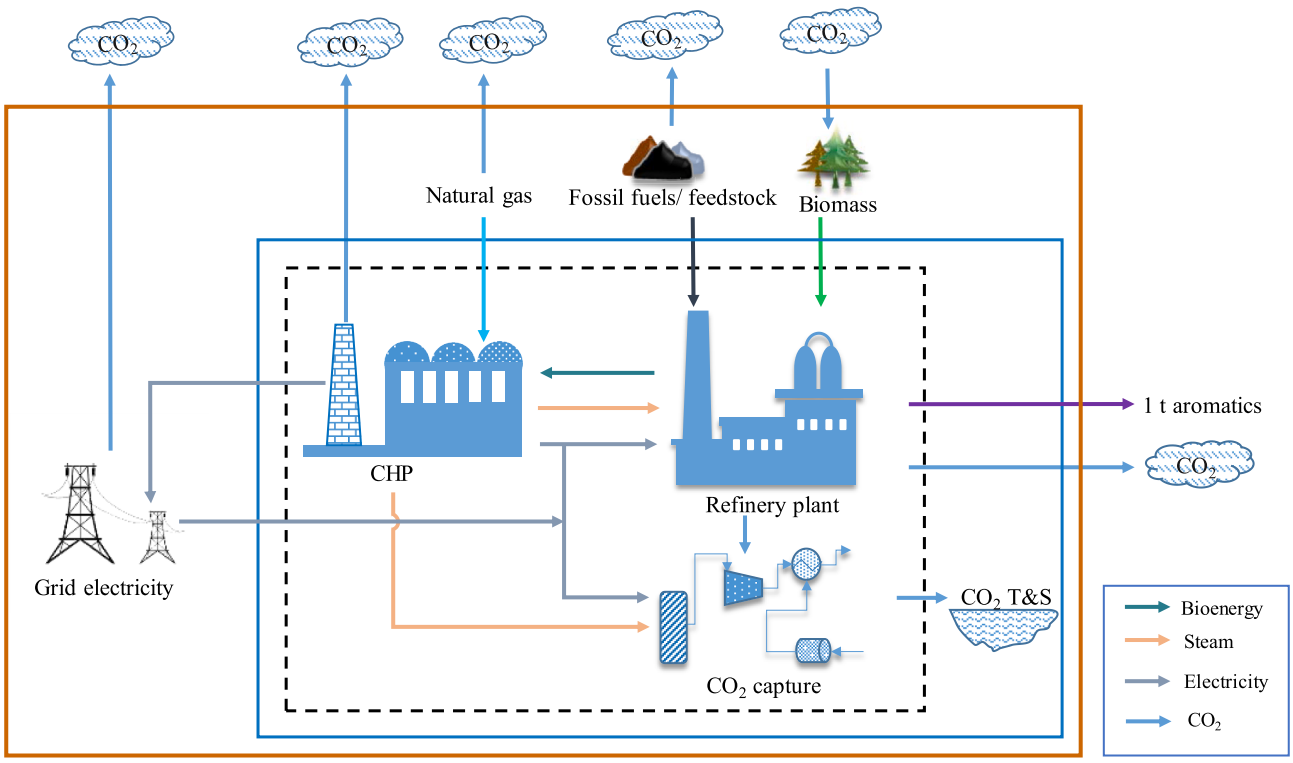

Fig. 2. System boundaries for aromatics industry. The black dotted box represents the aromatics production process model, the blue box represents the techno-economic evaluation, and the orange box represents the GHG emissions.

balanced with the electricity grid.

2.2. Performance indicators

The life cycle GHG emissions was calculated according to

$$GHG = GHG_{up} + GHG_{main} + GHG_{down} \quad (1)$$

where GHG (t CO_{2eq}/t aromatics) represents the life cycle CO_2 equivalent (CO_{2eq}) emissions from the industrial processes and GHG_{up}, GHG_{main}, and GHG_{down} (t CO_{2eq}/t aromatics) refer to upstream, main industrial process, and downstream emissions, respectively.

Applying Eq. (1) to aromatics production results in the follows:

$$GHG = \left[\sum F_i * Em_{CO_{2eq},up_i} + \sum F_i * X_i * \frac{44}{12} + E_{elec} Em_{elec} - F_{CO_2,c} * (1-\beta)\right] \Big/ F_p \quad (2)$$

where, for each raw material or energy carrier i, F_i (t/y or GJ/y) is the annual consumption of the raw material (t/y) or energy carrier (GJ/y); Em_{CO_2,up_i} (t CO_{2eq}/t or t CO_{2eq}/GJ) is the upstream CO_{2eq} emission factor (t CO_{2eq}/t or t CO_{2eq}/GJ); and X_i is the carbon content (t C/t or t C/GJ); 44/12 is the molar mass of CO_2 (44 kg/kmol) and C (12 kg/kmol), respectively; E_{elec} (GJ_e) is the electricity flow of the route[2]. Em_{elec} (t CO_2/GJ_e) is the CO_2 emission factor of the grid electricity; $F_{CO_2,c}$ (CO_2 t/y) is the amount of CO_2 captured; β is the fraction of the captured CO_2 lost during transport and storage; the downstream emissions represent the carbon contained in the aromatics; and F_P (t/y) is the annual aromatics production.

The avoided GHG emissions, $GHG_{avoided}$ (t CO_{2eq}/GJ), are calculated using Eq. (3), where GHG_{base} (t CO_{2eq}/GJ) and GHG_{case} (t CO_{2eq}/GJ) stand for the life cycle GHG emissions of the base case and the alternative cases, respectively.

$$GHG_{avoided} = GHG_{case} - GHG_{base} \quad (3)$$

The aromatics production cost ($/t aromatics), C_{BTX}, is calculated according to Eq. (4).

$$C_{BTX} = \left[\alpha * I + C_{O\&M} + C_{Feedstock} - \sum (F_{bpx} * C_{bpx}) + F_{CO_2,cap} * C_{T\&S}\right] \Big/ F_P \quad (4)$$

where α is the capital recovery factor (y^{-1}), calculated by $r/(1-(1+r)^{-L})$; r is the discount rate; L is the economic lifetime (y); I ($) is the total capital requirement (TCR); $C_{O\&M}$ ($/y) is the operating and maintenance costs; $C_{Feedstock}$ ($/y) is the feedstock cost; F_{bpx} (t/y) is the flow of by-product x; C_{bpx} ($/t) is the market price of by-product x; $C_{T\&S}$ ($/t) is the cost of transport and storage of CO_2; and C_{CO_2} ($/t) is the carbon price.

The GHG avoidance cost $C_{avoided}$ ($/t CO_{2eq}) is calculated by Eq. (5), where $C_{p,base}$ and $C_{p,case}$ represent production cost of the base case and alternative cases, respectively.

$$C_{avoided} = \left(C_{p,case} - C_{p,base}\right) / GHG_{avoided} \quad (5)$$

The total installed cost (TICs) of the individual components and/or production units were calculated and adjusted from the reported scale to the required scale using Eq. (6), with SF being the scaling factor.

$$Cost_{Case} \Big/ Cost_{Ref} = \left(Scale_{Case} / Scale_{Ref}\right)^{SF} \quad (6)$$

2.3. Standardization of key parameters

Key parameters were harmonized and standardized for a fair comparison through the following steps:

[2] This is the summation of the electricity consumption of main process and of the CO_2 capture and compression (if applicable) minus any electricity generated onsite. This also means that E_{elec} is negative when exporting electricity.

1 This study is an "N^{th}-of-a-kind" economic assessment that assumes that the technology is available at commercial scale and cost.
2 Wood chips were selected as the feedstock for the bio-based routes (Table 1). In the original literature, a variety of biomass types were used; however, the properties of these biomass types were similar to those of wood chips (Table S1). Additionally, the mass balance calculations were expressed on a dry basis; for the TGRP, CP, and HTL routes, the wood chips were dried from 30%wt to 4.5%wt (Chen et al., 2019; Elkasabi et al., 2014; Zheng et al., 2017). For GMA (Hu et al., 2011) and FFCA (Eerhart et al., 2014; Huijgen et al., 2011), the wood chips were dried from 30%wt to 12%wt and 10%wt moisture, respectively. Additionally, the chips were ground to <3 mm for all routes (Elkasabi et al., 2014; Mullen et al., 2013; Wright et al., 2010).
3 The energy and carbon contents and upstream GHG emission factors for the raw materials, mid-product, final product, and energy input were standardized as listed in Table 1. The GHG emissions from biomass collecting, harve sting, chipping, and transportation (assumed to be 100 km) were treated as upstream emissions (Miedema et al., 2017).
4 The distillation unit was assumed to be similar among different routes due to the lack of data. The aromatics amount in the biomass-oil before distillation are varied according to the different production processes (Details are shown in 3.2.1). The harmonized energy and carbon content of different biomass based oil were addressed in Table 1. The carbon content (88%) in the aromatics (Elkasabi et al., 2014) was assumed to be consistent. The remaining biomass-oil was treated as organic residues if there was no other specification. The recovery ratio of aromatics from the biomass-oil was assumed to be 100%.
5 All cost figures were converted to 2020 currency values ($\$_{2020}$) by first using year-averaged exchange rate data (for costs in other currencies), and then using the Chemical Engineering Plant Cost Index (CEPCI) (CEPCI, 2021). The key economic data is shown in Table 2.
6 The harmonized process plant and equipment costs are summarized in Table 3.

3. Production chains

This study describes conventional and alternative cases to produce aromatics. The starting point was aromatics produced from a conventional crude oil based refinery plant (BP, 2021; Oliveira and Schure, 2020) and the alternative routes with biomass and/or CCS. As there is no commercial bio-based aromatics plant, the biomass (dry basis) input was assumed to be 2000 t/day with annual operation hours of 8000 (Hu et al., 2011; Jones et al., 2013).

The input-output data of naphtha to aromatics and GMA case were based on, and adapted from, the simulation models in Aspen HYSYS, developed by Jiang et al. (2020). The mass and energy flow and reaction conditions of the other processes including crude oil to naphtha conversion, TRGP, CP, biomass to methanol, HTL, and FFCA were based on various previous studies (BP, 2021; Oliveira and Schure, 2020; Chen et al., 2019; Cheng and Huber, 2012; Eerhart et al., 2014; Elkasabi et al., 2014; Hu et al., 2011; Zheng et al., 2017).

The detailed technical data of the process flows are shown in the Table 4. Due to the requirements of the different production routes, the biomass pre-treatment includes drying and grinding (Miedema et al., 2017; Tews et al., 2014; Wright et al., 2010). The energy consumptions for each unit during aromatics production were based on the biofuel/biochemical production as they have similar reaction conditions and equipment (Eerhart et al., 2014; Hu et al., 2011; Tews et al., 2014; Thilakaratne, 2016). The reaction conditions and energy consumptions for the different routes and units are listed in Tables S2 and S3 in the Appendix.

All bio-based cases investigated in this study predominately produced BTX. The exception is the HTL case, which produces mainly derivatives of phenols and naphthalenes (sources); however, to perform

Table 1
Harmonized data regarding energy and content for key commodities.

Materials	HHV (GJ/t) [a]	C-content (%wt)	Upstream emissions (kg CO_2/GJ)	Sensitivity analysis
Natural gas [b]	56.9	74.0	24.9	6.2–43.6
Crude oil [c]	42.7	87.0	10.3	2.5–20.5
Wood chips [d]	20.3	50.1	23.6 kg CO_2/t	5.9–41.4
Cellulose [d]	18.7	44.4	/	/
Hemicellulose [d]	17.6	45.0	/	/
Lignin [d]	27	67.0	/	/
TGRP oil [e]	33.6	77.8	/	/
HTL oil [e]	39.8	85.3	/	/
CP oil [e]	30.0	68.0	/	/
DMF [e]	34.2	75.0	/	/
Furfural [e]	23.1	63.0	/	/
Methanol [e]	22.17	37.0	/	/
Biochar [e]	26.1	74.7	/	/
Aromatics [f]	38.5	87.7	/	/
Electricity [g]	/	/	224	3.6–342

[a] The unknown higher heating value (HHV) of feedstock or intermediate product is calculated by the following equation, based on the elemental composition: HHV (kJ/kg) = 35160 * C + 116225 * H - 11090 * O + 6280 * N + 10465 * S (Sami et al., 2001). If the lower heating value is known, but not the elemental composition, then a HHV:LHV ratio of 1:1 was assumed (Boschma and Kwant, 2013; Oliveira and Schure, 2020).

[b] The NG (dry basis) composition was assumed to be 83.9 vol% CH_4, 9.2 vol% C_2H_6, 3.3 vol% C_3H_8, 1.2 vol% C_4H_{10}, 0.2 vol% C_5H_{12}, 1.8 vol% CO_2, and 0.4 vol % N_2 (Hooey et al., 2013); this results in an energy density of 56.9 GJ_{HHV}/t and a carbon content of 74 wt%. The upstream emissions of domestic and imported NG in China are 6.2–38.9 kg CO_{2eq}/GJ and 14.5–43.6 kg CO_{2eq}/GJ according to prior studies (Gan et al., 2020; Zhang et al., 2021b). An average value of 24.92 CO_{2eq}/GJ was used in this study, and the range of 6.2–43.64 kg CO_{2eq}/GJ was used in sensitivity analyses.

[c] The energy and carbon contents of crude oil were based on prior research (Oliveira and Schure, 2020) and the upstream emissions were, likewise, based on prior research (Masnadi et al., 2018). The global upstream emissions ranged from 2.5 to 20.5 kg/GJ, and this range was used in the sensitivity analyses (Masnadi et al., 2018).

[d] The wood chips composition (C: 50.10%, H: 6.34%, O: 43.56%, and Ash: 0.03%) was based on the database of TNO (TNO, 2022). The ratio of cellulose, hemicellulose, and lignin of wood chips were 37.76%, 19.34%, and 36.8%, respectively, according to (Eerhart et al., 2014; Huijgen et al., 2011). The HHV of cellulose and hemicelluloses was approximately 17.5 GJ/t (Demirbas, 2017) and the HHV of lignin was 27 GJ/t (Demirbas, 2017; Paysepar, 2018). The upstream emissions from biomass harvesting, collecting, and chipping were 12.8 kg CO_{2eq}/t biomass, and the GHG emissions during biomass transportation were 0.096–0.121 kg CO_{2eq}/(biomass*km) (De Jong et al., 2017; Zhang, 2021). Here, a transportation distance of 100 km was assumed. The total upstream emissions of chips were 22.4–24.9 kg CO_{2eq}/biomass, with the average value used for the main calculations, and the value of 23.6 ± 75% was used in the sensitivity analyses.

[e] The energy and carbon contents of TGRP and HTL oils were based on previous (Chen et al., 2019; Mullen et al., 2013). The energy and carbon contents of CP oil were also based on previous studies (Vasalos et al., 2016; Zheng et al., 2017). The energy and carbon contents of DMF and furfural were calculated according to the chemical structure and the HHV calculation equation from a prior study (Sami et al., 2001). The energy and carbon contents of methanol and biochar were based on prior research (Hu et al., 2011; Paysepar, 2018).

[f] The energy and carbon contents of aromatics from TGRP were 38.5 GJ_{HHV}/t and 87.7%, respectively (Elkasabi et al., 2014). The aromatics selectivity of CP oil is 73.8%, and the energy and carbon contents of aromatics from CP route were 38.5 GJ_{HHV}/t and 91%, respectively (Zheng et al., 2017). The aromatics selectivity of HTL oil is 90% (Chen et al., 2019), and the energy and carbon contents of aromatics from the CP route were assumed to be similar to those of CP oil. The energy and carbon contents of aromatics from GMA were 43.4 GJ_{HHV}/t and 90.4%, respectively (Jiang et al., 2020).

[g] The GHG intensity of electricity is 0.744–861 kg/MWh in (Li et al., 2017a; Zhang et al., 2021b). An average electricity emission factor of 241.2 kg/MWh was used in this study. The GHG emissions of electricity generated from various sources, including fossil and biomass, range from 13.2 (hydropower) to 1230

kg/MWh (coal based power) (Feng et al., 2014). These values were used in the sensitivity analyses.

Table 2
Harmonized economic parameters.

Parameter	Unit	Value	Sensitivity analysis [e]
Economic lifetime [a]	year	20	/
Discount rate [a]	/	10%	/
Total plant cost [b]	% of TIC	130	/
Total capital requirement [b]	% of TPC	110	±30%
Operation and maintenance cost [c]	% of TCR	5.7	±30%
Labor cost [c]	% of TCR	1	±30%
Economic scaling factor [d]	/	0.67	/
Naphtha [e]	$/t	747.43	±30%
Wood chips [f]	$/GJ$_{HHV}$	8.84	6.27–11.40
Natural gas [g]	$/GJ$_{HHV}$	10.44	3.60–13.77
Electricity [h]	$/GJ	26.17	20.13–32.21
H_2 [i]	$/kg	3.42	±30%
LPG ($/t) [i]	$/t	812.40	±30%
Pentane ($/t) [i]	$/t	718.68	±30%
CO_2 transport and storage (T&S) cost [j]	$/t	13.05	10.80–77.63

[a] The economic life time and discount rate were consistent with Tews et al. (2014).

[b] Total installed costs (TIC) comprises both equipment and installation costs. TIC was 247% of total purchased equipment cost (TPEC) (Hu et al., 2011). The total plant cost (TPC) comprises IC, engineering fees, and contingencies; while the total capital requirement (TCR) comprises the TPC, owner costs, and interest during construction (Kuramochi et al., 2012). The total capital requirement was primarily calculated based on the costs associated with equipment and installation in the plant.

[c] Operation and maintenance costs (O&M) were estimated at 4%, 5%, and 8% of the TCR (Hu et al., 2011) and (Tews et al., 2014); an average O&M value of 5.7% was used for this study. The labor cost accounts for 1% of the TCR (Hu et al., 2011; Tews et al., 2014). Notably, all consumable costs were included in the O&M cost.

[d] Economic scaling factor was based on Berghout et al. (2019).

[e] The unit price of Naphtha was based on Jiang et al. (2020).

[f] The unit price of wood chips ranging from 6.21 to 11.4 $/GJ was based on Concawe et al. (Concawe, 2021) and the average valued was used in this study.

[g] The average natural gas price in China for industrial consumers in 2020 was 0.6 $/GJ (CEIC, 2020a). The average natural gas price in China for industrial consumers during 2010–2020 ranged from 7.85 to 13.77 $/GJ (CEIC, 2020a), and the imported natural gas price ranged from 3.6 to 13.3 $/GJ (Zhang et al., 2021b). These ranges were used in the sensitivity analyses.

[h] The average electricity price in China for industrial consumers in 2020 is 0.6 $/kWh (CEIC, 2020b).The average electricity price in China for industrial consumers during 2010–2020 ranged from 0.5 to 0.8 $/kWh (CEIC, 2020b). This range is used for the sensitivity analyses.

[i] An uncertainty range of ±30% was assumed for the sensitivity analysis if historic prices could not be found.

[j] The CO_2 T&S cost of 13.1 $/t was used according to (Yang et al., 2021a).

the technical analysis, it was assumed that HTL and CP oil are similar, which results in significant uncertainties in the outcome of the HTL case. Additionally, the technical analysis indicates that this case cannot reach negative emissions, even if CCS is applied. Therefore, the HTL case is not included in the economic evaluation.

3.1. NACR case (base case)

For the base NACR case, a conventional refinery plant adapted from existing refinery process units was used according to (BP, 2021; Oliveira and Schure, 2020). The process flow diagram is shown in Fig. 3 and Table S4 in the Appendix. The mass flow and composition of the products from crude oil distillation in China are based on the country level in 2020 (BP, 2021). The energy distribution for naphtha produced from crude oil was based on (Oliveira and Schure, 2020). A naphtha yield of

Table 3
The harmonized process plant total installed costs (TIC).

Process	Base scale	Unit	TIC (M $_{2020}$)
NACR [a]	0.45	Mt naphtha/y	15
MTA (methanol to aromatics) [a]	1.55	Mt methanol/y	10
Distillation (fossil route) [a]	0.45	Mt feed/y	15
Distillation (biomass route) [a]	1.55	Mt feed/y	24
Biomass grinder [b]	0.77	Mt biomass/y	2
Biomass dryer [b]	0.18	Mt water/y	14
TGRP [c]	0.66	Mt biomass/y	63
Catalytic pyrolysis unit [d]	0.72	Mt biomass/y	129
Hydrothermal liquefaction (HTL) [e]	0.72	Mt biomass/y	174
GTM (gasification to methanol) [f]	0.66	Mt biomass/y	195
Methanol-based organosolv [g]	0.63	Mt biomass/y	20
Primary sugar conversion [g]	0.63	Mt biomass/y	21
Furan conversion [g]	0.63	Mt biomass/y	3
Primary furfural recovery [g]	0.63	Mt biomass/y	7
Diels–Alder reactor [h]	0.72	Mt feed/y	129
Bio-oil filters [i]	0.66	Mt bio-oil/y	9
Water removal unit [j]	0.74	Mt water/y	11
Air separation unit (ASU) (fluidized bed) [k]	1839	t O_2/d	82
H_2 plant [l]	160	kt H_2/y	51
Onsite power plant [m]	215	MW_e	317
Steam boiler [m]	7.8	PJ/y	209

Note: Biomass for capital cost calculation was based on dry basis.

[a] The TIC of NACR, MTA, and distillation units were based on (Jiang et al., 2020).

[b] Particle size has been reduced from 10 mm to less than 3 mm by grinding (Wright et al., 2010). The TIC for the biomass grinder is 0.98 M$_{2010}$ (Wright et al., 2010), and it has a biomass capacity of 0.77 Mt/y. The TIC for the biomass dryer is 8.23 M$_{2010}$ with a water removal capacity of 0.18 Mt/y (Wright et al., 2010). The TICs for biomass grinder and dryer are 0.84 M$_{2012}$ and 1.06 M$_{2012}$, respectively, and their biomass capacity is 0.18 Mt/y and the water removal capacity is 0.01 Mt/y (Vasalos et al., 2016). Here, the average TIC of the biomass grinder was 2.4 M$_{2020}$ with a biomass capacity of 0.18 Mt/y, and that of the dryer was 11.4 M$_{2020}$ with annual removed water of 0.77 Mt.

[c] The TIC of FP is 162 M$_{2011}$ with capacity of 0.66 Mt/y dry biomass (Jones et al., 2013). The TIC of FP is 210 M$_{2014}$ with capacity of 0.58 Mt/y dry biomass (Tews et al., 2014). An average value of 202 M$_{2020}$ was used in this study. The TIC ratio of TGRP to FP is 31% (Sorunmu et al., 2017); therefore, the TIC of TRGP was 63 M$_{2020}$ in this study.

[d] The TIC of ex-situ CP equipment (including CP reactor/combustor, ex-situ catalytic vapor upgrading reactor/regenerator and heat integration) is 126.9 M$_{2012}$ with a capacity of 0.66 Mt/y dry biomass (Dutta et al., 2015).

[e] The TIC of HTL (including HTL reactor, wastewater treatment, and remainder OSBL) is 168.0 M$_{2008}$ with a capacity of 0.66 Mt/y dry biomass (Hu et al., 2011).

[f] The TIC of GTM (including directly-heated gasification with tar reforming, heat recovery, scrubbing, syngas clean-up and compression, methanol synthesis and separation, and remainder off-site battery limits (OSBL)) is 188 M$_{2008}$ (Hu et al., 2011).

[g] The TIC of methanol-based organosolv, primary sugar conversion, furan conversion and primary furfural recovery were adapted from (Eerhart et al., 2015).

[h] The TIC of the DA reactor (Cheng and Huber, 2012) is assumed to be the same as that of the CP reactor (Dutta et al., 2015) since both are fluidized beds.

[i] The TIC of the bio-oil filters was assumed to be the same for each bio-based route (Jones et al., 2013).

[j] The TIC of water removal unit was assumed to be consistent with (Zhang et al., 2021a).

[k] The capital cost of the ASU ranges from 34 to 147 M$_{2020}$ for 1839 t O_2/d (Hooey et al., 2013; Kuramochi et al., 2012; Meerman et al., 2012). The average value of 82 M$_{2020}$ was used in this study.

[l] The H_2 plant includes the sulfur guard bed, pre-reformer, steam methane reforming, water gas shift (WGS), pressure swing adsorption, compressors, and heat integration units (Dutta et al., 2015; Jones et al., 2013). The TIC of the H_2 plants ranged from 48 to 53 M$_{2020}$ with a capacity of 160 kt H_2/y.

[m] The TIC of onsite power plant and steam boil units were based on (Hooey et al., 2013).

Table 4
Harmonized technical results for different aromatics production route.

Route	Unit	NACR		TGRP		CP		HTL		GMA		FFCA	
		Base	CCS	Vent	CCS	Vent	CCS	Vent	CCS	Vent	CCS	Vent	CCS
Input													
Crude oil	t/t aromatics	13.68	13.68	/	/	/	/	/	/	/	/	/	/
Wood chips [a]	t/t aromatics	/	/	12.77	12.77	5.05	5.05	5.71	5.71	11.16	11.16	7.00	7.00
Fresh water [b]	t/t aromatics	/	/	/	/	/	/	/	/	14.88	14.88	27.27	27.27
Consumables [c]	t/t aromatics	/	/	/	/	1.01	1.01	3.43	3.43	2.80	2.80	1.39	1.39
Electricity	GJ/t aromatics	0.93	1.40	15.46	30.09	/	5.29	11.20	12.42	8.20	18.64	25.07	31.05
NG [d]	GJ/t aromatics	14.85	18.31	/	17.37	/	/	2.53	14.88	15.29	15.29	7.03	12.12
Output													
Aromatics	t/t aromatics	1.00	1.00	1.00	1.00	1.00	1.00	1.00	1.00	1.00	1.00	1.00	1.00
Residues	t/t aromatics	/	/	3.25	3.25	0.30	0.30	0.30	0.30	0.00	0.00	0.94	0.94
Wastewater	t/t aromatics	/	/	5.98	5.98	1.33	1.33	3.37	3.37	8.37	8.37	28.69	28.69
LPG [e]	t/t aromatics	0.47	0.47	/	/	/	/	/	/	1.01	1.01	/	/
Pentane	t/t aromatics	0.06	0.06	/	/	/	/	/	/	0.20	0.20	/	/
C6+ alkanes	t/t aromatics	0.22	0.22	/	/	/	/	/	/	/	/	/	/
Fuels from crude oil distillation [e]	t/t aromatics	9.65	9.65	/	/	/	/	/	/	/	/	/	/
H_2	t/t aromatics	0.06	0.06	/	/	/	/	/	/	/	/	/	/
Steam generation [f]	GJ/t aromatics	7.73	9.31	72.25	94.51	11.61	23.37	32.46	37.05	28.51	52.16	71.62	87.48
Electricity generation [f]	GJ/t aromatics	/	/	8.75	/	13.59	6.61	/	/	16.81	6.37	0.83	/
Electricity exported	GJ/t aromatics	/	/	/	/	4.20	/	/	/	/	/	/	/
Aromatics yield	/	7%	7%	7.8%	8%	20%	20%	18%	18%	9%	9%	14%	14%
GHG emissions	t CO_{2eq}/t aromatics	43.89	43.40	3.78	−2.13	−0.82	−3.82	2.84	1.37	3.27	−6.08	6.33	−1.07

[a] Dry basis of wood chips was used here for mass balance calculation. For TGRP, CP, and HTL, the wood chips were dried to 4.5% moisture; for GMA to 12%; and for FFCA to 10% moisture.
[b] This only includes the make-up water and not the recycled water.
[c] Consumables were assumed to be catalysts (Ga-ZSM-5) in the CP and(CuO and NaOH) HTL routes, purified O_2 (99.5%) in GMA route, methanol, H_2SO_4, catalyst, and butanol in the FFCA route. The consumables were not considered in the mass/energy distribution except for the electricity demand of the ASU.
[d] Natural gas was used to produce steam and/or hydrogen.
[e] This includes LPG from crude oil distillation and naphtha aromatization. The fuels from the crude oil distillation include gasoline, kerosene, diesel, and fuel oil.
[f] Onsite steam and electricity are generated from coke, NGCs, humins, and unreacted biomass.

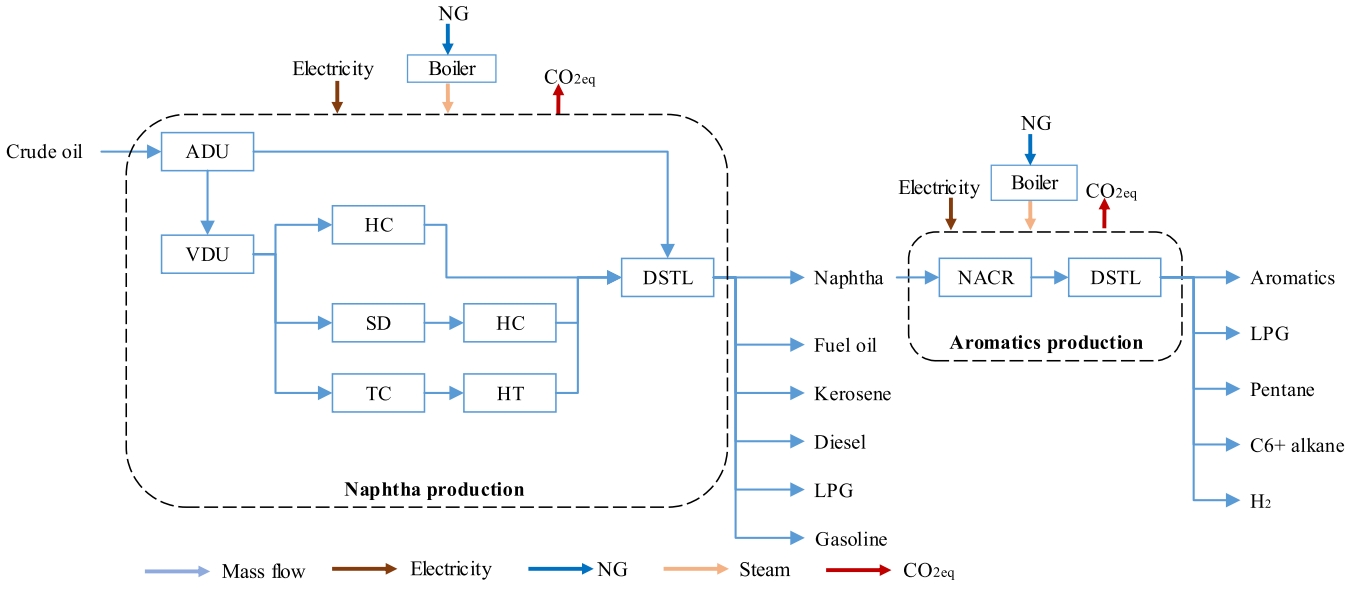

Fig. 3. Main production processes of the base case (Oliveira and Schure, 2020; Jiang et al., 2020) The blue and black boxes represent the main production unit and simplified energy consumption and CO_{2eq} emissions, respectively. The detailed process flow including mass, energy, and carbon flow is shown in Fig. S1 in the Appendix.

11%wt of the crude oil was used and the energy consumption of 0.67 GJ_{th}/t naphtha and 0.06 GJ_e/t naphtha was based on naphtha mass allocation from the conventional refinery plant (BP, 2021; Oliveira and Schure, 2020; Elgowainy et al., 2014; Wang et al., 2004). Other products included fuel oil, kerosene, diesel, Liquefied petroleum gas (LPG), and gasoline (BP, 2021).

The aromatics' yield of naphtha via catalytic reforming could reach 66%wt at 525 °C, 0.6 MPa (Jiang et al., 2020). Some onsite generated H_2 (6.3%wt naphtha) is recycled back to the reformer for the aromatization reaction (Jiang et al., 2020). The products then enter the distillation columns for aromatics extraction. The BTX and C9+ aromatic products account for 62% of the organics (Elkasabi et al., 2014). The remaining H_2 (3.9%wt naphtha), pentane (3.8%), C6+ alkanes (14.6%wt), and LPG (4%) are exported as by-products (Jiang et al., 2020).

ADU = Atmospheric distillation; VDU = Vacuum distillation; HC = Hydrocracking; SD = Solvent deasphalting unit; TS = Thermal cracking;

HT = Hydrotreating, DSTL = Distillation.

3.2. GHG mitigation options

The selected GHG mitigation options include substituting the fossil feedstock with biomass to produce aromatics and using biomass combined with CCS in the production processes.

3.2.1. Biomass cases

In this study, the main thermo-chemical conversion cases for producing aromatics from biomass that were evaluated were TGRP (Elkasabi et al., 2014), CP (Zheng et al., 2017), HTL (Chen et al., 2019), GMA (Hu et al., 2011; Jiang et al., 2020), and FFCA (Cheng and Huber, 2012; Eerhart et al., 2014). The distillation units were similar in all the cases based on (Jiang et al., 2020).

3.2.1.1. TGRP case. Usually, biomass is heated to 300–700 °C in an inert atmosphere to produce FP oil (Barik, 2019; Fernandez-Akarregi et al., 2013; Pinheiro Pires et al., 2019). FP oil needs to be upgraded in an H_2 atmosphere using zeolite catalysts at high pressure (Balagurumurthy et al., 2013). Compared to FP, TGRP uses a reductive atmosphere resulting in a stabilized oil without the need for H_2 or a catalyst (Elkasabi et al., 2014; Mullen et al., 2013; Sorunmu et al., 2017). TGRP oil is more stable, less acidic and richer in aromatics (Elkasabi et al., 2014; Mullen et al., 2013; Sorunmu et al., 2017). The aromatics can be separated via a fractional distillation unit similar to a conventional refinery plant (Elkasabi et al., 2014; McVey et al., 2020; Mullen et al., 2013).

In this study, the assumed TGRP process was broadly adapted from (Elkasabi et al., 2014), with a one-step pyrolysis oil yield of around 33% from wood chips. With this configuration, the feedstock was treated in the pyrolysis fluid bed reactor under 500 °C (Elkasabi et al., 2014); 52–58%wt liquid phase (including 32–36%wt oil and 16–23%wt water), 14–36%wt biochar, and 16–30%wt non-condensable gases (NCGs) were composed of the resulting (Elkasabi et al., 2014; Mullen et al., 2013). From the resulting vapors, the biochar was removed by a cyclone and the remaining liquid phases were condensed in a condensation train (Elkasabi et al., 2014), then the pyrolysis oil was collected from two electrostatic precipitators (ESPs) with recycled NCGs (Elkasabi et al., 2014). Usually, TGRP-oil is pyrolyzed with recycled tail-gas and shows optimal quality (Elkasabi et al., 2014, 2015; Mullen et al., 2013). Finally, the gas and oil products were separated and distilled by a three-phase separator and a train of distillation columns following previous procedures (Jiang et al., 2020). The aromatics content in the bio-based oil is 26%wt (Elkasabi et al., 2014). The remaining 74% of the TGRP oil without a specific composition is treated as the organic residue. The main aromatics components from the TGRP case are phenols and naphthalenes which account for 63%wt, while BTX only accounts for 7.9%wt (Elkasabi et al., 2014). The biochar and extra NCGs were assumed to provided heat to the system. Fig. 4 shows a process flow diagram of the TGRP case.

Unlike the atmosphere in fast pyrolysis, recycled gas provides a reductive atmosphere for the pyrolysis process which has the potential for higher aromatic biomass-oil yields (Mullen et al., 2013). Additionally, the undesired acidity and polymerization reactions are efficiently eliminated because the TGRP-oil contains lower oxygen (11–15%) than fast pyrolysis oil (15–35%) and catalytic pyrolysis oil (17–25%) (Elkasabi et al., 2014; Mullen et al., 2013). The TGRP-oil has lower total acid numbers, less water content, and higher energy content (33.2–35.8 MJ_{HHV}/kg) than fast pyrolysis oil (23.7–31.4 MJ_{HHV}/kg) and catalytic pyrolysis oil (29.7–32.3 MJ_{HHV}/kg) (Mullen et al., 2013).

3.2.1.2. CP case. CP uses a one-step reactor and does not require H_2. Aromatic yields are typically 5–22%wt_{dry} (Heeres et al., 2018; Paysepar, 2018; Yang et al., 2019b; Zheng et al., 2017). CP-based aromatic production is being tested in the Netherlands (Heeres, 2019) and in the USA (Anellotech, 2018, 2020). The feedstock is heated to 500 °C via a fixed-bed reactor, then the pyrolysis vapor is passed over the Ga-ZSM-5 catalyst to obtain the aromatics (Zheng et al., 2017); 25.8%wt CP oil, 26.4%wt water, 23.8%wt biochar, and 16–24%wt NCGs were produced during the process (Zheng et al., 2017). The aromatics selectivity of CP oil is 85.4%, which is mainly composed of 68.4% BTX and ethylbenzene (BTXE) and 17.0%wt naphthalene and its derivatives (Zheng et al., 2017). Fig. 5 depicts the conversion of wood chips to aromatics with catalytic pyrolysis technology (Jiang et al., 2020; Zheng et al., 2017).

3.2.1.3. HTL case. HTL is typically performed at 150–400 °C and at relatively high pressures (5–250 bar) (Cao et al., 2020; Chen et al., 2019; Gerssen-Gondelach et al., 2014; Gollakota et al., 2018; Jensen et al., 2017). In this study, the feedstock with mixture of homogeneous catalysts (NaOH) and heterogeneous catalysts (CuO) were assumed to be reacted at 230 °C with the maximum pressure of 2–8 MPa (Chen et al., 2019). The conversion ratio of feedstock is 86% and the yield distributions after HTL reaction were 26.6%wt HTL oil, 59%wt water, 14.4%wt biochar (Chen et al., 2019). The selectivity of aromatics in the HTL oil is 90%; however, there were no direct BTX products generated during this process (Chen et al., 2019). The composition of aromatics is very complex (49 compositions) and is mainly composed of the derivatives of phenols and naphthalene according to (Chen et al., 2019). To simplify the calculation, the modelled oil composition was assumed to be the same as that of CP. The NCGs less than 0.5%wt was neglected in this study (Chen et al., 2019), and the unreacted feedstock and biochar were assumed to be used as heat sources. A simplified process flow diagram of the HTL case for aromatics production is shown in Fig. 6.

3.2.1.4. GMA case. The main production processes of GMA case were divided to two parts and adapted from (Hu et al., 2011) and (Jiang et al., 2020). As described in Section 2.2, the biomass was first dried to a 12% wt moisture and a directly-heated gasifier was used to generate the syngas (Hu et al., 2011). Then the tar, light hydrocarbons, and methane were converted to H_2 and CO, with a H_2/CO ratio of approximately 2 with the imported fresh water in the steam reformer (Hu et al., 2011).

The methanol was synthesized in tubes with a ZnO/CuO catalyst at 278 °C and 5.86 MPa (Hu et al., 2011). To avoid the inert diluent (N_2) entering the syngas production system, an ASU was used to provide purified O_2 (99.5% purity) to the reaction (Hu et al., 2011). The purge gas from methanol synthesis was used as fuel for the production system (Hu et al., 2011). Natural gas (1.37 GJ/t dry feedstock) was used to supplement the requirement of the plant fuel gas[4] (Hu et al., 2011). The product allocation according to dry feedstock is 46%wt methanol accompany, with 64%wt flue gas and 73%wt of CO_2 (Hu et al., 2011). Here, the CO_2 means the directly emitted CO_2 after syngas cleaning throughout the CO_2 removal amine unit (Hu et al., 2011). The high quantity of steam produced from methanol production and the aromatization reactor were used for steam and power generation (Hu et al., 2011; Jiang et al., 2020).

The second part is the methanol reacting at 230 °C and a pressure of 0.4 MPa in the aromatization reactor; the aromatics yield is 19.4%wt and the by-product yield is 19.6%wt (LPG) and 3.9%wt (pentane) (Jiang et al., 2020). The modelled aromatics are mainly composed of BTX and C9+ aromatics (Jiang et al., 2020). The flue gas from the methanol production process and NCGs from the aromatization process were used

[3] For all the flow diagrams in this study, the mass and carbon losses (if there is any) were allocated to wastewater, which is not shown in the diagrams.

[4] Natural gas can be substituted by recycled gas produced from the methanol synthesis, but this will lower the methanol yield (Hu et al., 2011). To avoid of lowering the methanol yield and further reducing the aromatics yield, this study used natural gas as supplemental heat sources.

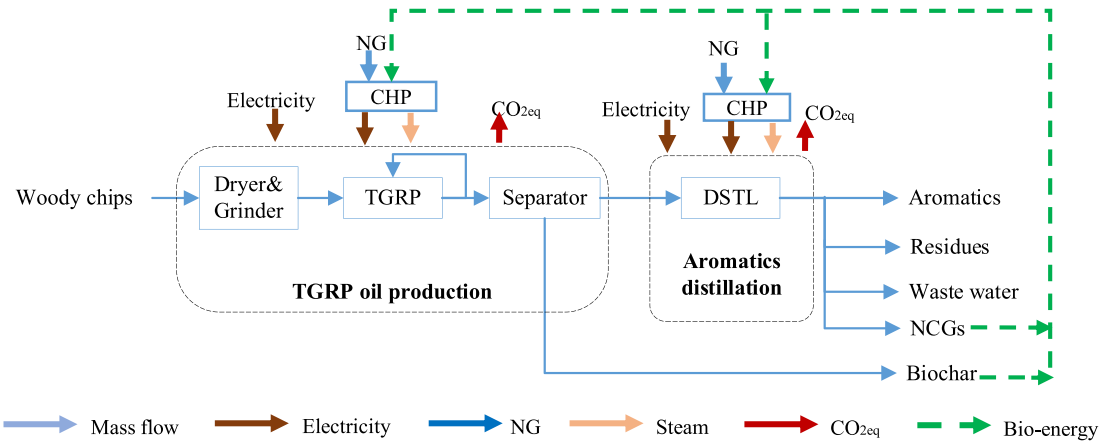

Fig. 4. Main production processes of the TGRP case[3] (Elkasabi et al., 2014; Jiang et al., 2020).The blue and black boxes represent the main production unit and the simplified energy consumption and CO_{2eq} emissions, respectively. The detailed process flow including mass, energy, and carbon flow is shown in Fig. S2 in the Appendix.

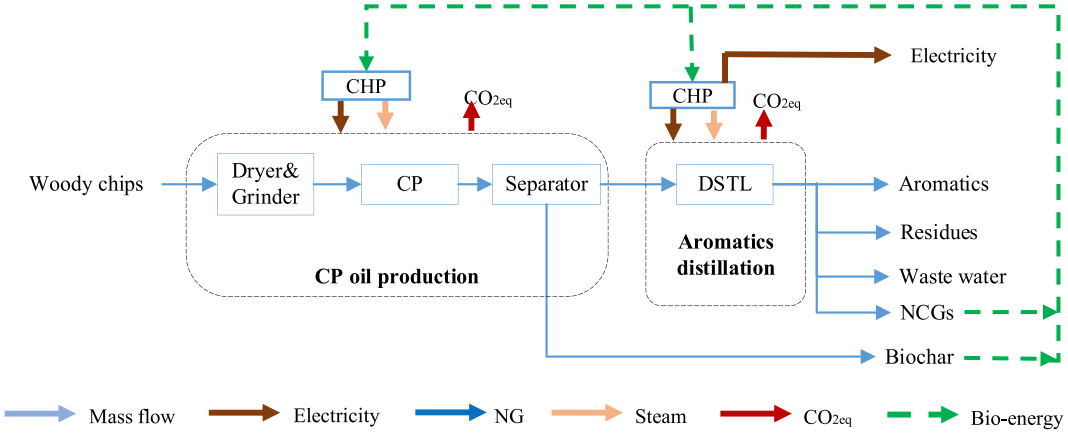

Fig. 5. Main production processes of CP case (Jiang et al., 2020; Zheng et al., 2017). The blue and black boxes represent the main production unit and the simplified energy consumption and CO_{2eq} emissions, respectively. The detailed process flow including mass, energy, and carbon flow is shown in Fig. S3 in the Appendix.

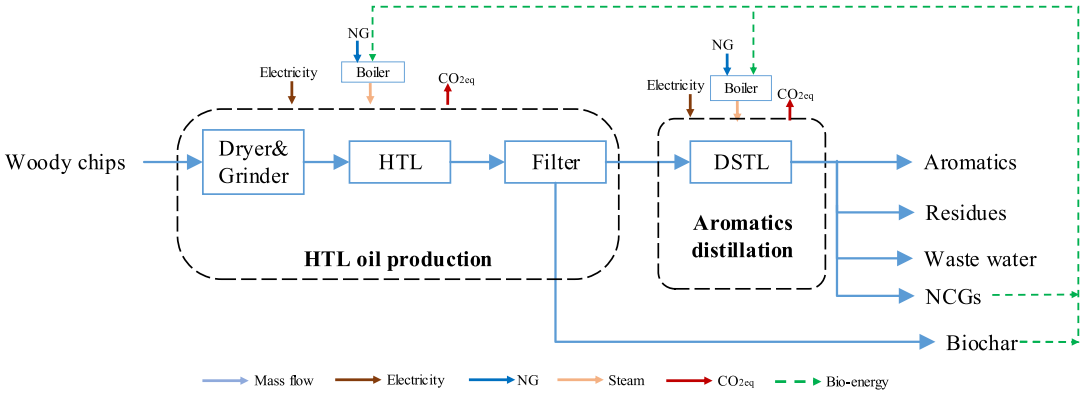

Fig. 6. Main production processes of HTL case (Chen et al., 2019; Jiang et al., 2020). The blue and black boxes represent the main production unit and the simplified energy consumption and CO_{2eq} emissions, respectively. The detailed process flow including mass, energy, and carbon flow is shown in Fig. S4 in the Appendix.

as onsite heat sources. The main process flow of GMA case is shown in Fig. 7.

3.2.1.5. FFCA case. For the bio-chemical conversion, furan compounds are extracted from biomass via enzymatic (Dos Santos et al., 2019; Eerhart et al., 2014; Luo et al., 2019; Yan et al., 2014). Pretreatment, whether carried out at acidic, neutral or alkaline conditions, or in ionic fluids, involves dissolving and/or hydrolyzing the hemicellulose fractions, and removing 10–50% of the lignin. The resulting solid material is rich in cellulose, still contains significant amounts of lignin, poor in hemicellulose and almost devoid of extractives and ash (Dos Santos et al., 2019). The furans are converted into aromatics using Diels–Alder cycloaddition and aromatization (Cheng and Huber, 2012; Wijaya et al., 2016). Lignin can be converted to either power (Eerhart et al., 2014) or

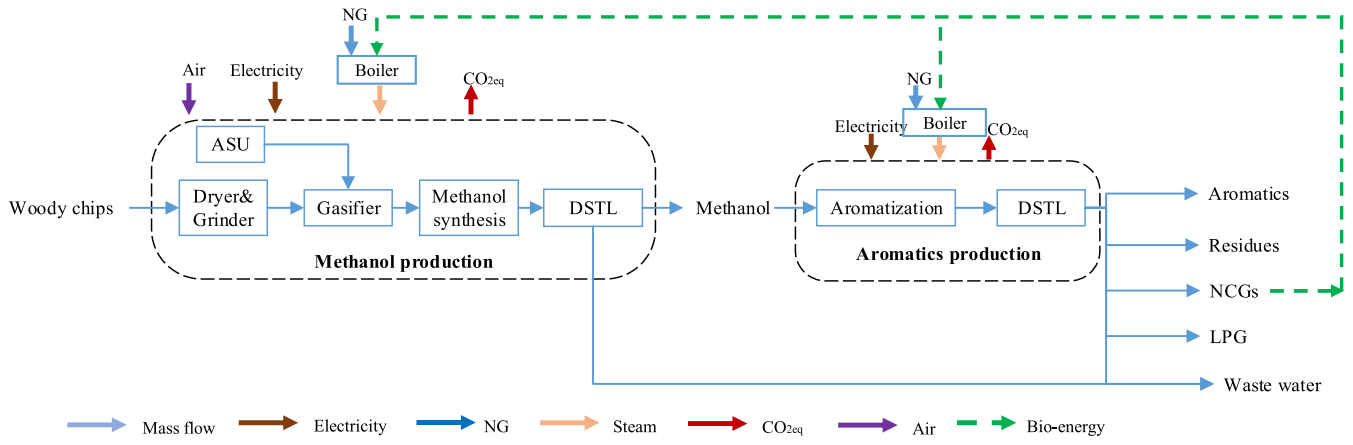

Fig. 7. Main production processes of GMA case (Hu et al., 2011; Jiang et al., 2020). The blue and black boxes represent the main production unit and the simplified energy consumption and CO_{2eq} emissions, respectively. The detailed process flow including mass, energy, and carbon flow is shown in Fig. S5 in the Appendix.

aromatics via CP/HTL (Paysepar, 2018).

In this study, the cellulose, hemicellulose, and lignin conversion cases were combined for an integrated bio-refinery. Organosolv fractionation allows for the recovery of the three primary lignocellulosic biomass constituents (cellulose, hemicellulose, and lignin) (Eerhart et al., 2014). The biomass uses an aqueous methanol solution (60% methanol) for organosolv fractionation, which was carried out at 200 °C for 60–80 min at 3 MPa (Eerhart et al., 2014). The main process flow of aromatics produced from FFCA case is depicted in Fig. 8.

Cellulose was first converted to glucose (94%wt of cellulose) via enzymatic hydrolysis (Eerhart et al., 2014), then the glucose was converted to fructose (71%wt glucose) by acid-catalyzed dehydration, and then to HMF (62%wt fructose) by dehydration (Eerhart et al., 2014; Li et al., 2016). Next, HMF is converted to DMF via hydrogenolysis with H_2 injection (3%wt fructose) and a catalyst (Roman-Leshkov et al., 2007). The H_2 was assumed to have been generated by imported NG with the steam generated onsite (Berghout et al., 2019). Finally, DMF (46%wt fructose) was recovered and converted to a biomass-oil rich in aromatics by the Diels–Alder reaction and dehydration (Cheng and Huber, 2012).

The hemicellulose portion of the biomass produces high yields of xylose (80%wt) through hydrolysis (Green, 2014). The xylose was used as the feedstock for furfural compounds (38%wt xylose) (Eerhart et al., 2014), which were converted to produce biomass-oil rich in aromatics via the Diels–Alder reaction and the aromatization processes (Cheng and Huber, 2012). In this study, the lignin (72%wt extracted yield) was used for aromatics production via CP (Eerhart et al., 2014; Paysepar, 2018) and the mid-products from the lignin catalytic pyrolysis were composed of CP oil (25.8%wt), wastewater (26.4%wt), biochar (23.8%wt), and NCGs (20.2%wt) (Paysepar, 2018). The residue stream, humins, biochar, NCGs, and unreacted lignin were then burned in the boiler to provide heat and power (Eerhart et al., 2014).

EAH = Enzymatic hydrolysis for cellulose; ACDH = Acid-catalyzed dehydration for hemicellulose; DACE = Diels–Alder reactor for cellulose; DAHE = Diels–Alder reactor for hemicellulose case.

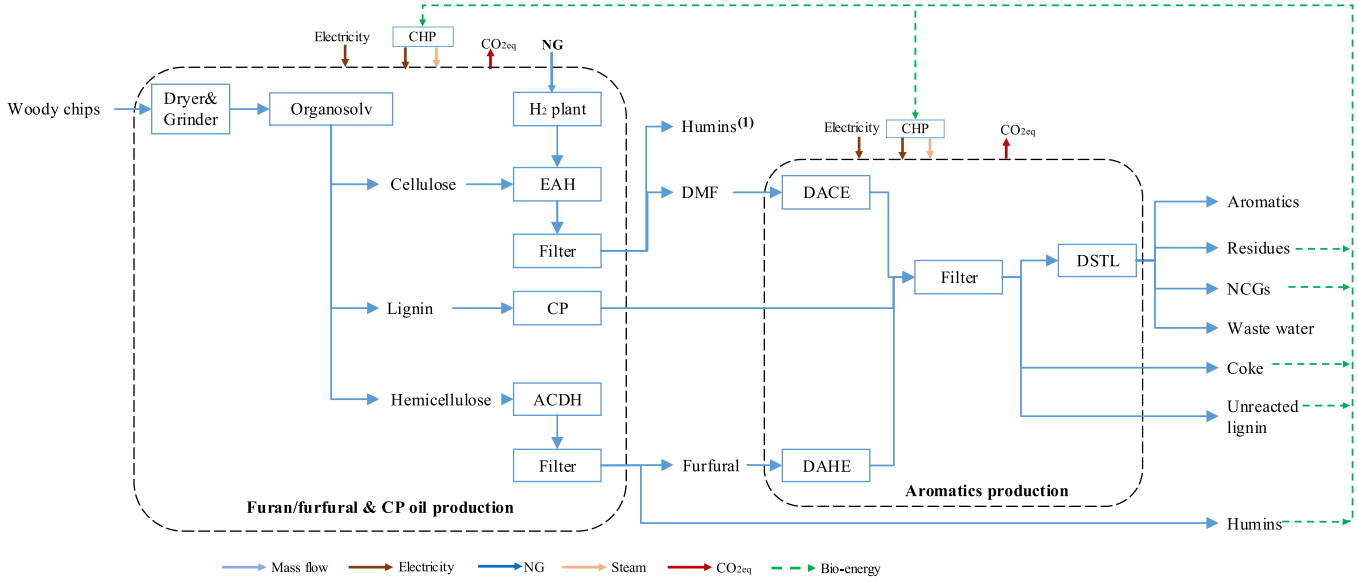

Fig. 8. Main production processes of FFCA case (Cheng and Huber, 2012; Eerhart et al., 2014; Green, 2014; Li et al., 2016). The blue and black boxed represent the main production unit and the simplified energy consumption and CO_{2eq} emissions, respectively. The detailed process flow including mass, energy and carbon flow is shown in Fig. S6 in the Appendix

Note: The humins(1) from cellulose enzymatic hydrolysis were also used for onsite steam and electricity generation.

3.2.2. Carbon capture and storage

3.2.2.1. NACR with CCS case. The base case was adapted for CO_2 capture by adding post-combustion CO_2 capture using the commercial MDEA/Pz solvent (40% MDEA and 10% Pz) (Hooey et al., 2013). The capture ratio is 90% and uses 2.27 GJ_{th}/t CO_2 and 0.6 GJ_e/t CO_2 regardless of flue gas composition (Hooey et al., 2013). CO_2 capture was applied to all the CO_2 emission processes, including the in situ steam boiler unit, and the CO_2 emissions from the increased energy demand due to CO_2 capture were also evaluated. After drying, cooling, and

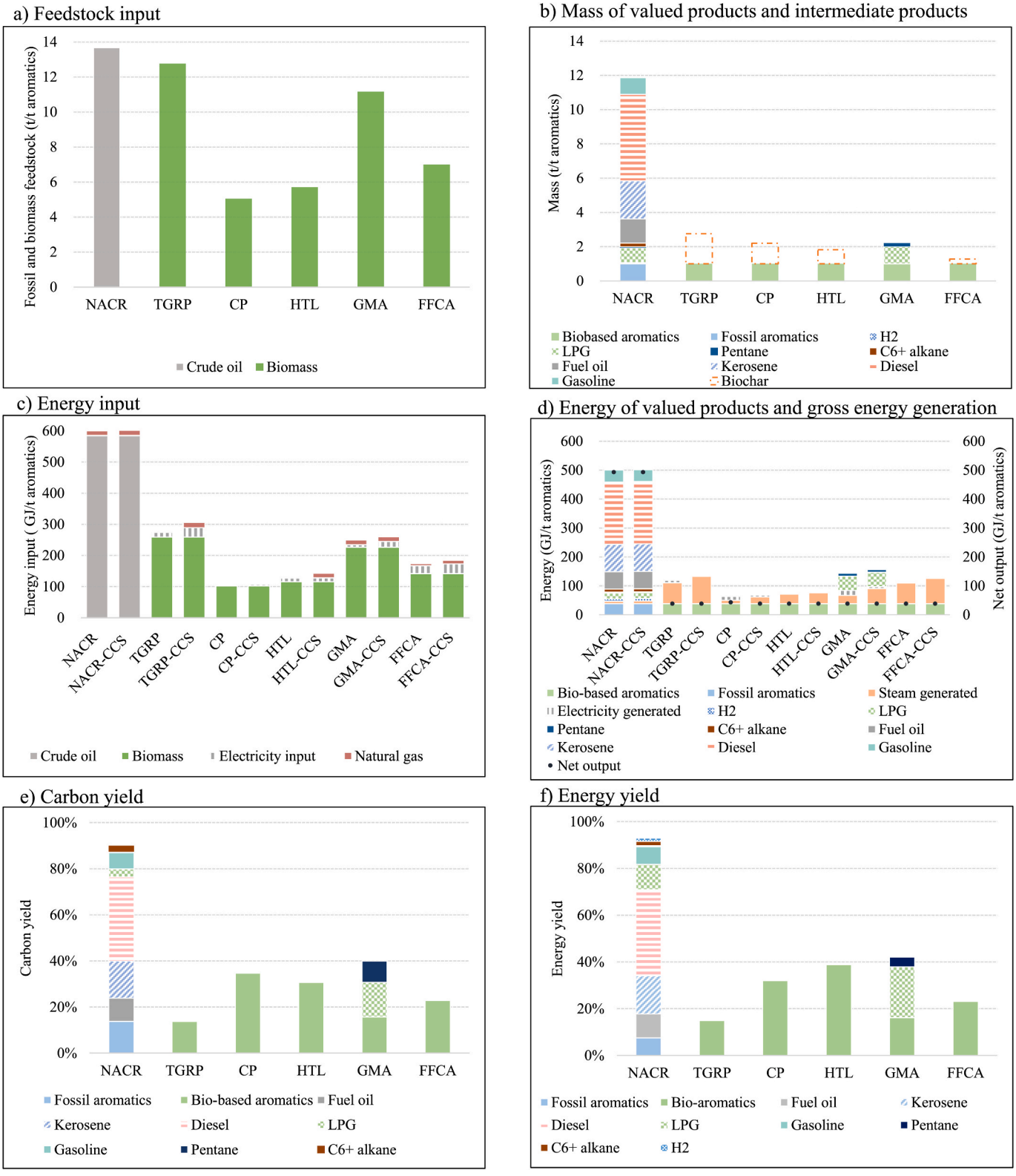

Fig. 9. Technical results of different production routes. a) Feedstock input — biomass is dry basis. b) NCGs and wastewater excluded. c) The energy content of crude oil is 43 GJ_{HHV}/t. d) The net outputs include chemical products and electricity (only for CP). e) and f) The carbon and energy yields of valued products.

purifying, the captured CO_2 is compressed to 110 bar for transport to the storage site. For all CCS cases, the emission ratio of the transported CO_2 accounts for 1% of the captured CO_2 based on 100 km pipeline (Metz et al., 2005). As the capture process is an add-on process, no effect on aromatics yield was assumed.

3.2.2.2. BECCS cases. BECCS is the combination of bio-based aromatics production cases and CCS. The main mass flow was the same in the cases without CCS. The energy consumption, NG, and electricity imported were adapted for all the CCS cases. The process energy was used for producing more steam to supply the capture unit. Only the CP-CCS route produced enough bioenergy for onsite electricity generation. The detailed process flows of all the CCS/BECCS are shown in Figs. S7–S12 in the Appendix.

4. Results

4.1. Mass and energy of aromatics production cases

The results show large variations in aromatics mass and energy yields between the tested cases (Fig. 9 and Table 4). The aromatics yield (7%wt crude oil) in the base case is lower than those in the biomass related cases (8–23%wt dry biomass) (Fig. 9(a) and (b)). However, none of the biomass options are competitive with the valued product yields of the base petroleum case because 89%wt of the crude oil is converted to transportation fuels. In contrast, more than 75%wt of the biomass is converted to wastewater, NCGs, and biochar/coke. Among the biomass options, the single step CP and HTL cases show higher aromatics yields than the multi-step GMA and FFCA cases due to the conversion losses in each step.

For the energy comparison, the situation differs from the mass comparison. The base case, which produces the most valued products, contains the highest energy content (Fig. 9 (c) and (d). Significant differences are found regarding steam and/or power generation. The FFCA case has the highest energy from combustible by-products (92.8 GJ/t aromatics); however, due to the energy-intensive conversion, this energy is primarily used for steam generation and only a small part of the electricity requirement is satisfied. Meanwhile, the CP case exports the highest amount of electricity (4.2 GJ/t aromatics). Results also show that the carbon yield of the biomass cases is low (<40%) and most of the carbon embedded in the feedstock is emitted as CO_2 (Fig. 9 (e) and (f)). This makes these cases good candidates for CCS.

The energy consumption for each unit was then compared (Fig. 10 (a) and (b)). The total specific thermal energy (7.73 GJ_{th}/t aromatics) and electricity (0.91 GJ_e/t aromatics) consumption in the base case are lower than those in the other cases. The energy integration from naphtha to aromatics compensates a part of the imported energy. Additionally, as aromatics are by-products from crude oil refinery plants, a significant part of the energy consumption is allocated to the large quantity of by-products. Lastly, the high aromatics yield from the naphtha catalytic reforming contributes to the low energy consumption. Within the biomass cases, the energy consumption is comparable; therefore, the high CP case yields result in the lowest specific energy consumption (−4.2 GJ_e/t aromatics). Conversely, the low yield of the TGRP case results in the highest specific energy consumption of 24 GJ_e/t aromatics and 78 GJ_{th}/t aromatics. The pre-treatment processes, which are primarily composed of drying, grinding, and organosolv fractionating, are the most energy intensive units. The energy consumption in the main reactors depends on the process configurations. Generally, the more reaction steps, the higher the energy consumption. For the distillation columns, the specific energy consumption in the base case is the highest because it requires energy for H_2 recovery and alkanes separation; this requirement is not applicable to the biomass options.

4.2. GHG emissions mitigation of aromatics production cases

The base case, the CCS cases, and all the biomass cases with and without CCS were compared in terms of their ability to lower GHG emissions (Fig. 11). The base case has life cycle GHG emissions of 43.9 t CO_{2eq}/t aromatics. CCS has a very limited effect on GHG mitigation for

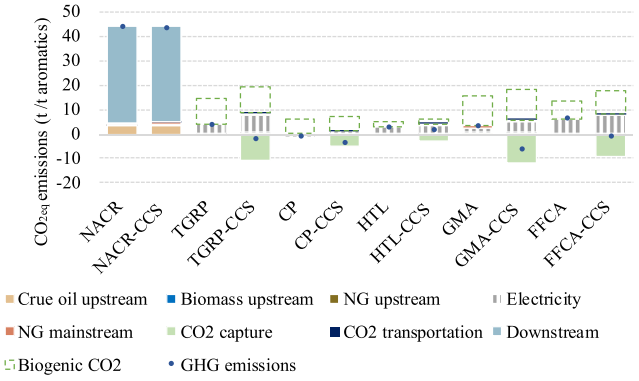

Fig. 11. The GHG emissions distributions in each production route.

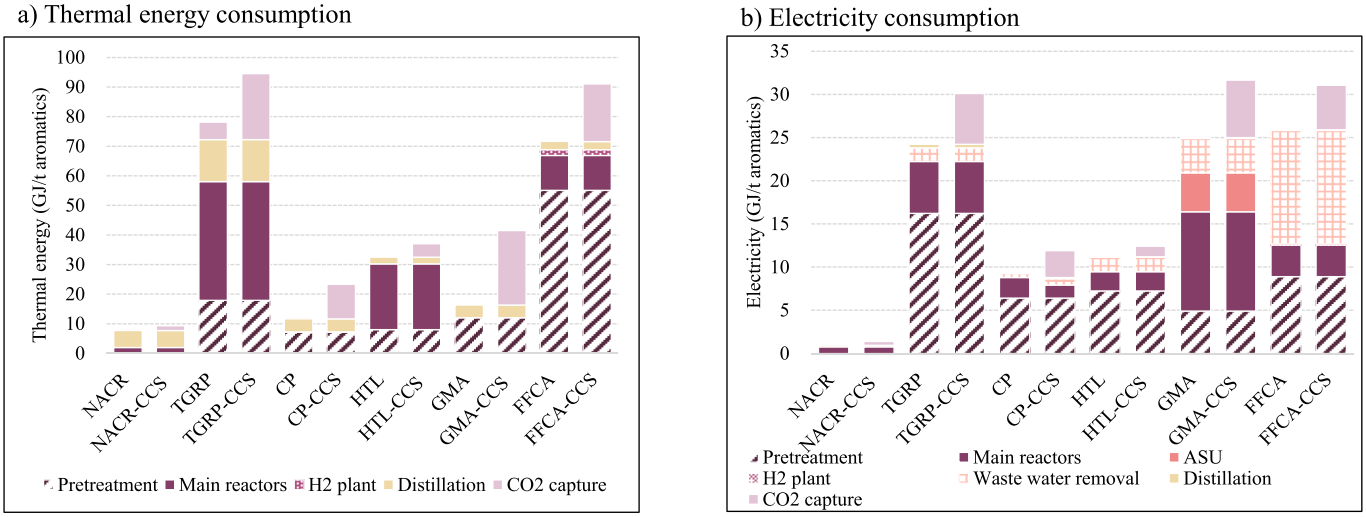

Fig. 10. Thermal (a) and electricity (b) consumption.

the base case as most of the carbon is embedded in the aromatics or by-products, while all of the biomass cases show significant GHG reductions and FFCA shows the highest GHG emissions of 6.33 t CO_2/t aromatics. The CP case already has negative emissions (−0.82 t CO_{2eq}/t aromatics) without CCS because of the exported electricity; the credits received for this export offset the upstream emissions of the biomass. Regarding all the biomass cases, the GHG mitigation potential ranges from 86% (FFCA) to 102% (CP). For the BECCS cases, the more CO_2 generated onsite, the higher the CO_2 capture potential and the lower the final life cycle GHG emissions. As a result, all the BECCS cases reach negative emissions except for HTL-CCS. The GMA case has the highest onsite CO_2 emissions (12.33 t CO_{2eq}/t aromatics), which consists of direct CO_2 from methanol production, flue gas from syngas production, and NCGs from methanol aromatization. Consequentially, the CCS potential for GMA is significant, and the GMA-CCS case results have the lowest GHG emissions (−6.08 t CO_{2eq}/t aromatics) of all investigated cases.

4.3. Aromatics production costs and GHG avoidance costs

The production costs of CCS, biomass, and BECCS cases were compared to the cost of the base case (Fig. 12). The results show a wide variation in production costs, ranging from 1077 to 5371 $/t aromatics; however, none of the cases are cost competitive with the base case (1077 $/t aromatics). Since the capital cost in the base case only includes the processes for converting naphtha to aromatics, the TCR of the base case (392 $/t aromatics) is much lower than those of the bio-based cases (464–995 $/t aromatics). Additionally, the base case also produces a substantial amount of valuable by-products, further decreasing the aromatics production cost.

For the biomass cases, energy generation units and the main reaction equipment are the main contributors to the TCR. TIC differences between the cases can be explained by the differences in equipment type, cost, and scale. TGRP shows the highest production cost due to the combination of high TCR, low yield, and limited by-products sales. The CP case has the lowest bio-based production cost due to its high yield, electricity export, and low capital cost. For the BECCS cases, the increased capital costs are mainly from the CO_2 capture unit and a subsequent increase in size of the steam boilers; this also means that there is less steam available for electricity production, resulting in a smaller power plant.

The avoided costs for different aromatics cases were compared (Fig. 13). The life cycle GHG emissions of NACR-CCS was 43.4 t CO_{2eq}/t aromatics, corresponding to the lowest avoided ratio of 1% CO_{2eq}, wherein the CO_{2eq} avoidance cost is 136 $/t CO_{2eq}. CP shows the lowest avoidance cost of 22 $/t CO_{2eq} and TGRP shows the highest avoidance cost of 85.9 $/t CO_{2eq} due to the highest production cost and the second highest GHG emissions. TGRP-CCS and GMA-CCS show the highest avoidance costs of 93.3 $/t CO_{2eq} and 74.4 $/t CO_{2eq}, respectively, due to the low yield of aromatics. The GHG avoidance costs for CP-CCS are the lowest (27.6 $/t CO_{2eq}) with GHG emissions of −3.8 t CO_{2eq}/t aromatics. These results are comparable to the levelized cost of CO_2 capture in industrial sectors (<120 $/t CO_{2eq})[5] (IEA, 2019b).

4.4. Sensitivity analysis of aromatics production cases

All CCS, biomass, and BECCS cases were chosen for sensitivity analyses. The parameters included changes to the NG prices, electricity prices, naphtha prices, wood chip prices, by-product prices, CO_2 T&S prices, capital costs, NG upstream emission intensities, electricity, crude oil, and wood chips (Tables 1 and 2).

[5] The levelized cost of CO_2 capture from the bioethanol production, or SMR which produces the high concentrated CO_2 streams, is 15–35 $/t CO_{2eq} and from the processes with less concentrated CO_2 streams 40–120 $/t CO_{2eq} (IEA, 2019b).

The GHG avoidance cost of NACR-CCS is the most sensitive to changes in economic parameters (Fig. 14). In NACR-CCS, the avoidance cost is more affected by the naphtha and by-product prices with the uncertainty range of ± 30%. According to this, the GHG avoidance cost of NACR-CCS can be reduced from 135.7 to −369.1 $/t CO_{2eq}; however, the GHG avoidance costs of the biomass options are more sensitive to the capital cost and the OPEX (Fig. S13 in the Appendix). This can be explained by that CAPEX and OPEX accounting for 36–63% of the production costs. The avoidance costs of the GMA and GMA-CCS cases drop the most (32 $/t CO_{2eq}) in the lower limit cases; for the lowest avoidance cost options (CP and CP-CCS), the avoidance cost could drop from 22.0 $/t CO_{2eq} and 27.6 $/t CO_{2eq} to 8.2 $/t CO_{2eq} and 13.3 $/t CO_{2eq}, respectively. With the uncertainty range of 83–595%, the avoidance costs of BECCS are sensitive to the upper limit of CO_2 T&S price.

For the integrated analyses of all cost parameters, the GHG avoidance cost in the NACR-CCS case could drop to −693.4 $/t CO_{2eq}. Under favorable conditions for the BECCS cases, CP-CCS and TGRP-CCS represent the best and worst options with avoidance costs of 8.2 $/t CO_{2eq} and 58.9 $/t CO_{2eq}, respectively. Under the worst conditions, the avoidance cost of NACR-CCS (944 $/t CO_{2eq}) is much higher than that of the BECCS options (35.8–140.7 $/t CO_{2eq}).

With an uncertainty range for upstream emission intensities of natural gas (26–184%), electricity (1–152%), crude oil (45–455%), and wood chips (25–175%), the GHG avoidance cost of NACR-CCS represents the option which was most sensitive to upstream emissions due to the lowest production cost variations among all the cases (Fig. 15). The avoidance cost drops from 136 $/t CO_{2eq} to 23.2 $/t CO_{2eq} under favorable conditions. Under the worst conditions, the GHG emissions in NACR-CCS are higher than those in NACR, because the upstream emissions were unchanged in the base case. For the biomass options, the effects of the upstream intensities of NG and wood chips are very limited (Fig. S14 in the Appendix). Only the TGRP and TGRP-CCS cases with the lowest aromatics yields are sensitive to the upstream emissions of wood chip, with avoidance costs of 77.0 $/t CO_{2eq} and 84.7 $/t CO_{2eq} under the lower limit. With the high electricity import, TGRP-CCS and FFCA-CCS were more sensitive to upstream electricity intensities. Under favorable conditions in the combination of the upstream intensities, TGRP-CCS and FFCA-CCS show the greatest decrease in avoidance costs.

The combination results of costs and upstream emissions show that NACR-CCS is the most sensitivity (Fig. 16). Under favorable conditions, the avoidance cost of NACR-CCS is −119 $/t CO_{2eq} with GHG emissions of 41.0 t CO_{2eq}/t aromatics. The biomass options show avoidance costs of 8.0–44.4 $/t CO_{2eq}, in the biomass cases, and 12.3–47.0 $/t CO_{2eq}, in the BECCS cases, with GHG emissions ranging from −4.24 to −1.71 t CO_{2eq}/t aromatics and from −6.9 to −14.6 t CO_{2eq}/t aromatics, respectively. The sensitivity analysis also indicates that the CP and CP-CCS routes keep having the lowest CO_2 avoidance cost of the biomass cases.

5. Discussions

This study extensively investigated and compared aromatics produced from various technologies and addressed the techno-economic performance of bio-based aromatics value chains. These results are subject to uncertainties according to the available data quality and the related assumptions made for different routes (Table 5). The process flows, including mass, energy and carbon balances, production costs, and GHG avoidance costs were based on a literature review. The availability and quality of this data varied for the different cases.

The data quality of the mass balances is better than that of the others parameters because most studies are still in the laboratory exploration stage and as such heat integration and process scales are not yet optimized. The aromatics yields were based on various production routes with different feedstock; however, to simplify the calculations and make the comparison among the routes possible, the biomass feedstock (wood

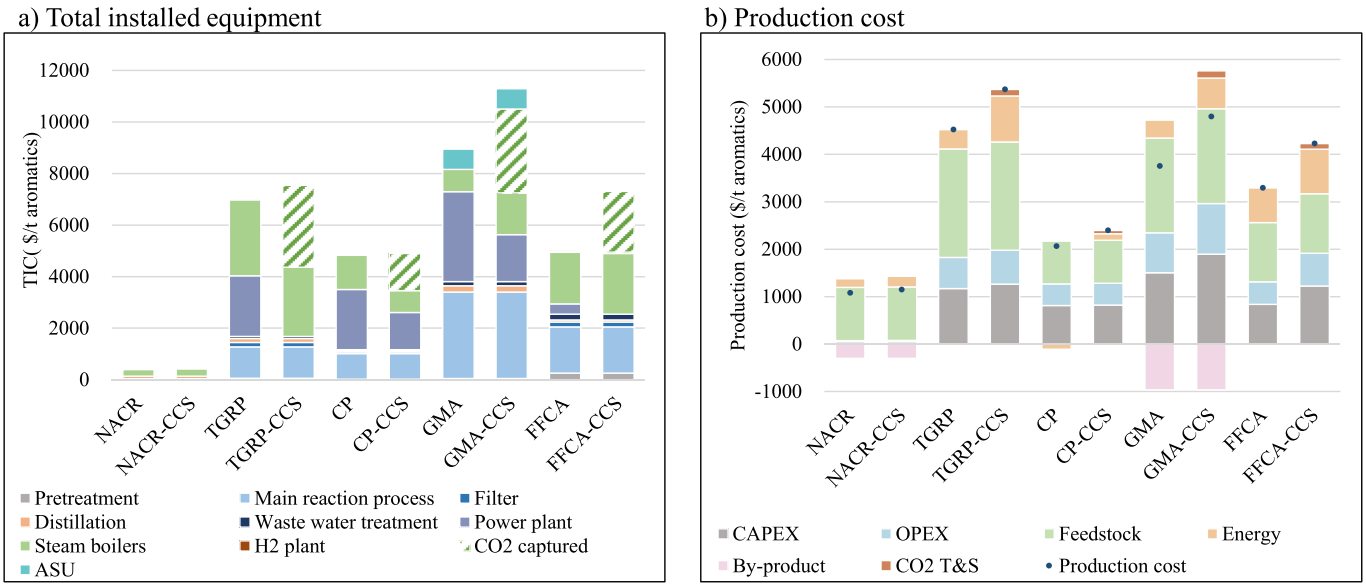

Fig. 12. TIC and production cost compositions for different aromatics cases. The detailed information is shown in Table S5 in the Appendix.

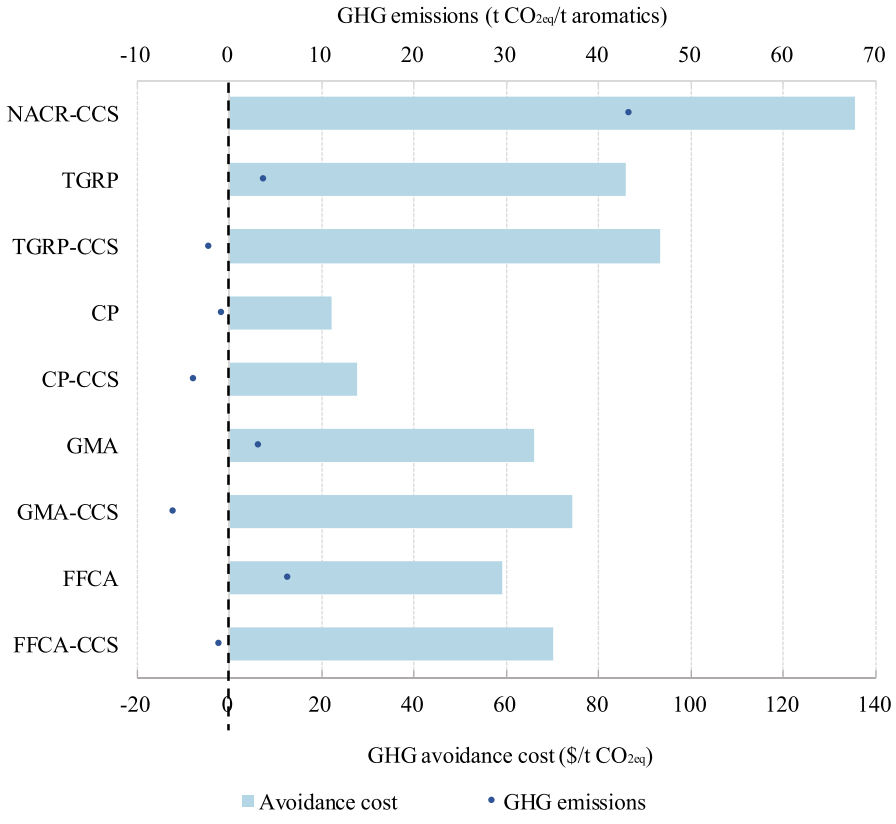

Fig. 13. GHG emissions and avoidance costs for difference cases.

chips) used in this study was very case specific. Although the various lignocellulosic biomass categories had similar properties to each other, there remain uncertainties during practical production.

Without a scaled-up production, the energy consumptions during the production processes were mainly adapted from the biofuel or biochemical production which had similar reactions, equipment, and utilities with bio-based aromatics. The combined heat and power generation for increasing the energy efficiency has been proven in the industrial sectors (Hooey et al., 2013). As this study does not include detailed modelling work of aromatics production routes, the energy integration in this study used literature-based assumptions. The MTA and base case distillations were adapted from literature (Jiang et al., 2020). For other processes, there was a lack in literature-based estimation and optimization and the energy consumption and generation were only estimations.

As the bio-oil compositions were not consistent in each case, there

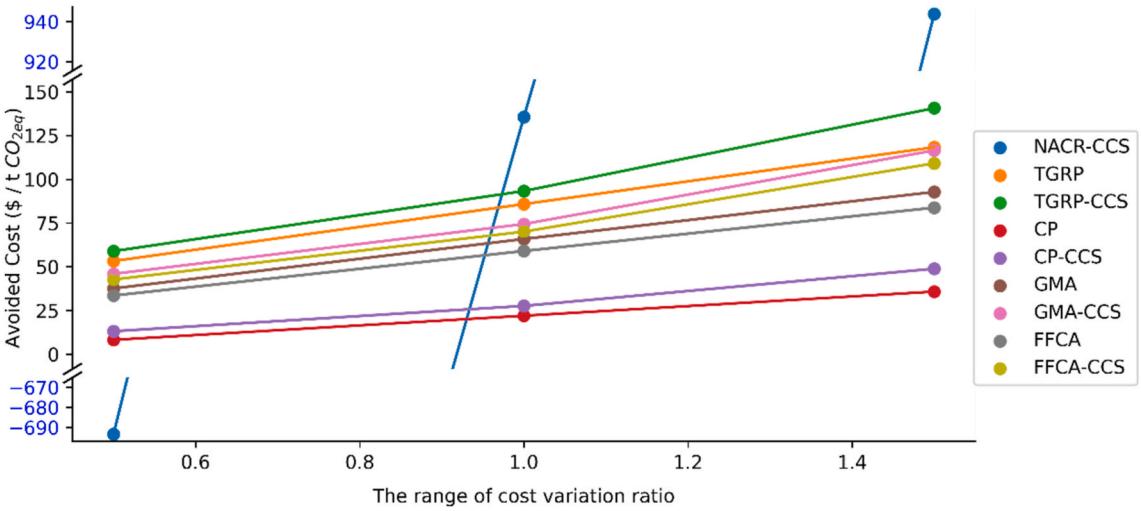

Fig. 14. The combined costs sensitivity analysis. The combination option includes all cost related factors (feedstock, energy input, by-products, CO_2 transport, and storage and capital cost). The decimal number presents the ratio of lower and upper limits to the cases without sensitivity.

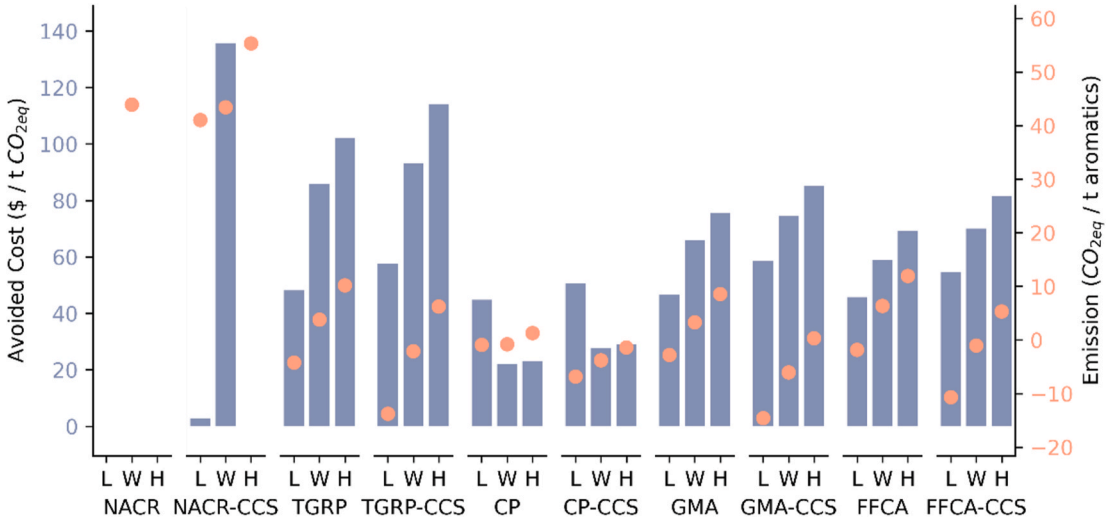

Fig. 15. The combined upstream emissions sensitivity analyses. L = GHG avoidance cost with lower limit, W = without sensitivity, U = upper limit.

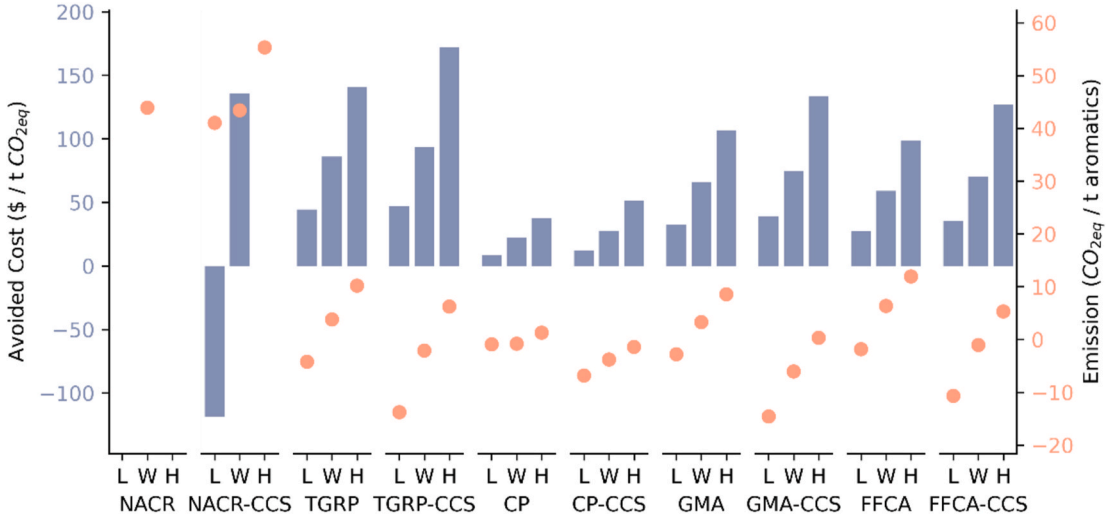

Fig. 16. The combination of cost sensitivity and upstream emissions sensitivity analyses. L = GHG avoidance cost with lower limit, W = without sensitivity, U = upper limit.

Table 5
Data quality evaluation for different aromatics production.

	TGRP			CP			HTL		
	Mass	Energy	Cost	Mass	Energy	Cost	Mass	Energy	Cost
Pretreatment									
Reaction									
Distillation									
Utility									
Integration									
Overall									
	GMA			FFCA			Legend		
	Mass	Energy	Cost	Mass	Energy	Cost	Data quality		
Pretreatment							High	Medium	Low
Reaction									
Distillation									
Utility									
Integration									
Overall									

were uncertainties during the calculations. The utility was also adapted from literature data; however, as there is no harmonization for utilities, the energy consumption may differ from similar units. For the biomass routes, the mass and energy flows were often constructed from different literature sources due to unavailability of data.

The lack of cost data for the available routes affected the selection of value chains for economic evaluation. The pre-treatment processes for biomasses have existed as commercial technology for a substantial amount of time and such data are robust. The main processes, however, are not yet commercially available and their efficiency, scale and capital cost were estimated based on analogue processes. As there is no accurate capital cost published for crude oil to naphtha conversion, a wholesale market naphtha price was used to represent the processes cost. The investment costs for the equipment required for the biomass routes are rather uncertain. Not all of the technologies have been realized at the commercial scale and most of them are still in the laboratory (Chen et al., 2019; Eerhart et al., 2014; Elkasabi et al., 2014; Hu et al., 2011; Jiang et al., 2020; Zheng et al., 2017).

Due to the complexity of the HTL oil composition, the distillation could have large variations on energy consumption compared to aromatics from methanol. Therefore, the energy consumption and cost estimation for HTL is relatively unreliable. The FFCA case is a concept design based on current aromatics synthesis technologies from the individual composition of lignocellulosic biomass, and there might be several uncertainties during the integration productions. The mass and energy flow for the furans production part was roughly estimated from a modelling plant which produce PEF and FEE (Eerhart et al., 2014). The detailed energy consumption and integration for each reaction unit are unknown. The cost is assumed and calculated based on the feedstock, energy equipment and utility, and therefore, less reliable than the mass and energy calculations.

As there is no explicit energy consumption and cost data for most biomass aromatics productions, the energy and cost date are primarily obtained from modelling work or biofuel productions with similar equipment. Therefore, the data for biomass options is less robust in the technology sector than the economic sector. The GHG avoidance cost was dependent on the production costs and GHG emissions mitigation potentials. These results are comparable to the CO_2 capture cost in industry (25–120 $/t CO_{2eq}) (IEA, 2019b).

The comparison result between literature and this study shows that the aromatics production cost of the base case (1076 $/t) was lower primarily due to the valued by-products from crude oil not included in the reference route (Table 6). All the production costs of the biomass cases (2060–4520 $/t) are in the cost ranges of the literature except for that of the TGRP case. The wide range in costs can be explained by the various feedstock types, conversion yield and reactions, and equipment and utilities.

Besides dedicated bio-refineries, there is the option to co-process bio-oil with petroleum mid-products in conventional refineries (Fogassy et al., 2010; Ng et al., 2019; Pinho et al., 2015; Yáñez et al., 2021). A limited number of studies have focused on co-processing bio-BTX production (Elkasabi et al., 2014; McVey et al., 2020; Yáñez et al., 2021). As the bio-oil is injected for bio-fuel co-processing in the refinery production units, the bio-BTX production routes are assumed to be similar to bio-fuel routes. Based on previous studies, the co-procession positions could be distillation units for TGRP oil (Elkasabi et al., 2014; McVey et al., 2020), fluid catalytic cracking (FCC) units for catalytic pyrolysis bio-oil or vegetable (Al-Sabawi et al., 2012; Balagurumurthy et al., 2013; He et al., 2018), and hydrotreating units for vegetable oil (Al-Sabawi and Chen, 2012). However, co-refining is not yet commercial available; for example, co-processing 20% CP oil in an FCC has only been demonstrated at the laboratory scale (TRL 4–5) (Pinho et al., 2015), and at 10% in a demonstration stage (TRL 7) (Pinho et al., 2017). Using biomass gasification and co-processing pyrolysis oil in the hydrotreating unit is even more experimental at TRL 3–6 (Gudde et al., 2019). Co-processing bio-aromatics in conventional refineries could decrease production cost of bio-aromatics by; retrofitting existing refinery infrastructure, increasing stability and quality of the bio-oils, overcoming scaling problems, and decreasing logistics costs.

6. Conclusion

In this study, the techno-economic performance of bio-based aromatics value chains were investigated and compared to the conventional

Table 6
The production cost comparison results from literature review.

Products	Production cost ($/t)	Feedstock	Route	Reference
BTX	1457	Naphtha	Catalytic reformer	Jiang et al. (2020)
P-xylene	4121	Starch	Catalytic conversion	Lin et al. (2014)
P-xylene	1480–2420	Lignocellulosic biomass	Hydrolysis process	Athaley et al. (2019)
BTX	2083	Methanol	Aromatization	Jiang et al. (2020)
Aromatics	1950	Lignin	Depolymerization	(Vural Gursel et al., 2019)
Aromatic-rich hydrocarbons	1577–1949	Lignocellulosic biomass	Thermochemical conversion	Corredor et al. (2019)

production routes using a harmonized methodology. Using key technical parameters, capital and feedstock costs, and the carbon intensities for different processes and materials, the production costs, GHG emissions, and GHG avoidance costs of different production routes were calculated.

The base case shows the lowest production cost of 1077 $/t aromatics at an oil price of around 60 $/barrel, with low CAPEX (46 $/t aromatics) and feedstock costs (1125 $/t aromatics). Among the biomass options, CP shows the lowest production cost (2061 $/t aromatics). This also means that if naphtha prices roughly double, the CP case becomes cost-competitive with the base case. BECCS cases show more GHG emission reduction potential (103–116%) than biomass options (87–102%) with a comparable GHG avoidance cost.

For the sensitivity analyses, the combined impact of uncertainties in feedstock (both fossil and biomass), CO_2 transport prices and capital cost have a linear impact on the economic performance for all the options. The avoidance cost of CP remained the lowest and all the BECCS cases could reach an avoidance costs of 50 $/t CO_{2eq} or lower. NACR-CCS cases are more sensitive to feedstock prices while the biomass options are more sensitive to the capital cost and OPEX. Under the worst conditions, with the highest upstream emissions, the GHG emissions from NACR-CCS (55.1 t CO_{2eq}/t aromatics) are higher than those of the base case (43.9 t CO_{2eq}/t aromatics) and, therefore, it is counterproductive to apply CCS. However, this is an extreme case and unlikely to happen.

The bio-based aromatics production routes investigated in this study can be used to compensate the expected decline in petroleum-based aromatic production. Results indicate that negative emissions can be achieved for the BECCS cases at CO_2 avoidance costs of under 100 $/t CO_{2eq}. This would imply that bio-based aromatics production can be an important option for the deployment of large-scale projects with negative emissions and relatively low CO_2 avoidance costs. Based on this study, GMA-CCS, which has the lowest GHG emissions, and CP, which has the lowest avoidance cost, should be investigated further to validate the results given here and to gain operational experience in producing bio-aromatics.

CRediT authorship contribution statement

Fan Yang: Conceptualization, Methodology, Formal analysis, Investigation, Visualization, Writing – original draft. **Hans Meerman:** Methodology, Validation, Writing – review & editing. **Zhenhua Zhang:** Data curation, Software, Visualization. **Jianrong Jiang:** Resources, Software. **André Faaij:** Conceptualization, Supervision, Writing – review & editing.

Declaration of competing interest

The authors declare that they have no known competing financial interests or personal relationships that could have appeared to influence the work reported in this paper.

Data availability

Data will be made available on request.

Acknowledgements

This work is supported by China Scholarship Council and University of Groningen (award to Fan Yang for 4 years of study at the University of Groningen).

Appendix A. Supplementary data

Supplementary data to this article can be found online at https://doi.org/10.1016/j.jclepro.2022.133727.

References

AFC TCP, 2018. Survey on the Number of Fuel Cell Vehicles. Hydrogen Refueling Stations and Targets.
Al-Sabawi, M., Chen, J., 2012. Hydroprocessing of biomass-derived oils and their blends with petroleum feedstocks: a review. Energy Fuel. 26, 5373–5399. https://doi.org/10.1021/ef3006405.
Al-Sabawi, M., Chen, J., Ng, S., 2012. Fluid catalytic cracking of biomass-derived oils and their blends with petroleum feedstocks: a review. Energy Fuel. 26, 5355–5372. https://doi.org/10.1021/ef3006417.
Anellotech, 2018. Commercializing Bio-Paraxylene to Make 100% Bio-Based PET Bottles a Reality. NewYork.
Anellotech, 2019. Anellotech New Sustainable Solution to Create Basic Aromatic Chemicals and Olefins from Recycled Plastic Waste. NewYork.
Anellotech, 2020. Renewably Sourced Chemicals for Virgin Bio-Packaging February 2020 Plastics Chemical Recycling. NewYork.
Athaley, A., Annam, P., Saha, B., Ierapetritou, M., 2019. Techno-economic and life cycle analysis of different types of hydrolysis process for the production of p-Xylene. Comput. Chem. Eng. 121, 685–695. https://doi.org/10.1016/j.compchemeng.2018.11.018.
Balagurumurthy, B., Oza, T.S., Bhaskar, T., Adhikari, D.K., 2013. Renewable hydrocarbons through biomass hydropyrolysis process: challenges and opportunities. J. Mater. Cycles Waste Manag. 15, 9–15. https://doi.org/10.1007/s10163-012-0097-2.
Barik, D., 2019. Energy from Toxic Organic Waste for Heat and Power Generation. Rapid Prototyping of Biomaterials - Techniques in Additive Manufacturing. Elsevier. https://doi.org/10.1016/C2017-0-01876-1.
Bender, M., 2013. Global aromatics supply - today and tomorrow, 2013 DGMK - Tagungsbericht 59–65.
Berghout, N., Meerman, H., van den Broek, M., Faaij, A., 2019. Assessing deployment pathways for greenhouse gas emissions reductions in an industrial plant – a case study for a complex oil refinery. Appl. Energy 236, 354–378. https://doi.org/10.1016/j.apenergy.2018.11.074.
Bielansky, P., Weinert, A., Schönberger, C., Reichhold, A., 2011. Catalytic conversion of vegetable oils in a continuous FCC pilot plant. Fuel Process. Technol. 92, 2305–2311. https://doi.org/10.1016/j.fuproc.2011.07.021.
Boschma, S., Kwant, I.K.W., 2013. Valorization of Palm Oil (Mill) Residues. Identifying and Solving the Challenges. NL Agency, Utrecht.
BP, 2020. Energy Outlook. BP, London.
BP, 2021. Statistical Review of World Energy 2021, BP Energy Outlook 2021. London.
Cao, Y., Zhang, C., Tsang, D.C.W., Fan, J., Clark, J.H., Zhang, S., 2020. Hydrothermal liquefaction of lignin to aromatic chemicals: impact of lignin structure. Ind. Eng. Chem. Res. 59, 16957–16969. https://doi.org/10.1021/acs.iecr.0c01617.
CEIC, 2020a. China natural gas price [WWW Document]. URL. https://www.ceicdata.com/en/china/gas-price-36-city, 12.5.21.
CEIC, 2020b. China electricity price [WWW Document]. CEIC. URL. https://www.ceicdata.com/en/china/electricity-price-36-city, 12.6.21.
CEPCI, 2021. The chemical engineering plant cost index—chemical engineering [WWW Document]. URL. http://www.chemengonline.com/pci-home, 9.1.21.
Chen, H., Shi, X., Liu, J., Jie, K., Zhang, Z., Hu, X., Zhu, Y., Lu, X., Fu, J., Huang, H., Dai, S., 2018. Controlled synthesis of hierarchical ZSM-5 for catalytic fast pyrolysis of cellulose to aromatics. J. Mater. Chem. 6, 21178–21185. https://doi.org/10.1039/C8TA08930B.
Chen, Y., Dong, L., Miao, J., Wang, J., Zhu, C., Xu, Y., Chen, G.Y., Liu, J., 2019. Hydrothermal liquefaction of corn straw with mixed catalysts for the production of bio-oil and aromatic compounds. Bioresour. Technol. 294, 122148 https://doi.org/10.1016/j.biortech.2019.122148.
Cheng, Y.T., Huber, G.W., 2012. Production of targeted aromatics by using Diels-Alder classes of reactions with furans and olefins over ZSM-5. Green Chem. 14, 3114–3125. https://doi.org/10.1039/c2gc35767d.
Concawe, 2021. Sustainable biomass availability in the EU. to 2050 [WWW Document]. URL. https://www.concawe.eu/publication/sustainable-biomass-availability-in-the-eu-to-2050/.
Corredor, E.C., Chitta, P., Deo, M.D., 2019. Techno-economic evaluation of a process for direct conversion of methane to aromatics. Fuel Process. Technol. 183, 55–61. https://doi.org/10.1016/j.fuproc.2018.05.038.
De Jong, S., Antonissen, K., Hoefnagels, R., Lonza, L., Wang, M., Faaij, A., Junginger, M., 2017. Life-cycle analysis of greenhouse gas emissions from renewable jet fuel production. Biotechnol. Biofuels 10, 64. https://doi.org/10.1186/s13068-017-0739-7.
De Wild, P.J., Huijgen, W.J.J., Gosselink, R.J.A., 2014. Lignin pyrolysis for profitable lignocellulosic biorefineries. Biofuels, Bioprod. Biorefining 8, 645–657. https://doi.org/10.1002/bbb.1474.
Demirbas, A., 2017. Higher heating values of lignin types from wood and non-wood lignocellulosic biomasses. Energy Sources, Part A Recover. Util. Environ. Eff. 39, 592–598. https://doi.org/10.1080/15567036.2016.1248798.
Dos Santos, A.C., Ximenes, E., Kim, Y., Ladisch, M.R., 2019. Lignin–enzyme interactions in the hydrolysis of lignocellulosic biomass. Trends Biotechnol. 37, 518–531. https://doi.org/10.1016/j.tibtech.2018.10.010.
Duan, P., Savage, P.E., 2011. Hydrothermal liquefaction of a microalga with heterogeneous catalysts. Ind. Eng. Chem. Res. 50, 52–61. https://doi.org/10.1021/ie100758s.
Dupain, X., Costa, D.J., Schaverien, C.J., Makkee, M., Moulijn, J.A., 2007. Cracking of a rapeseed vegetable oil under realistic FCC conditions. Appl. Catal. B Environ. 72, 44–61. https://doi.org/10.1016/j.apcatb.2006.10.005.

Dutta, A., Sahir, A., Tan, E., Humbird, D., Snowden-swan, L.J., Meyer, P., Ross, J., Sexton, D., Yap, R., Lukas, J., 2015. Process Design and Economics for the Conversion of Lignocellulosic Biomass to Hydrocarbon Fuels. NREL.

Eerhart, A.J.J.E., Huijgen, W.J.J., Grisel, R.J.H., Van Der Waal, J.C., De Jong, E., De Sousa Dias, A., Faaij, A.P.C., Patel, M.K., 2014. Fuels and plastics from lignocellulosic biomass via the furan pathway; A technical analysis. RSC Adv. 4, 3536–3549. https://doi.org/10.1039/c3ra43512a.

Eerhart, A.J.J.E., Patel, M.K., Faaij, A.P.C., 2015. Fuels and plastics from lignocellulosic biomass via the furan pathway: an economic analysis. Biofuels, Bioprod. Biorefining 9, 307–325. https://doi.org/10.1002/bbb.1537.

Elgowainy, A., Han, J., Cai, H., Wang, M., Forman, G.S., Divita, V.B., 2014. Energy efficiency and greenhouse gas emission intensity of petroleum products at U.S. Refineries. Environ. Sci. Technol. 48, 7612–7624. https://doi.org/10.1021/es5010347.

Elkasabi, Y., Mullen, C.A., Boateng, A.A., 2014. Distillation and isolation of commodity chemicals from bio-oil made by tail-gas reactive pyrolysis. ACS Sustain. Chem. Eng. 2, 2042–2052. https://doi.org/10.1021/sc5002879.

Elkasabi, Y., Mullen, C.A., Boateng, A.A., 2015. Aqueous extractive upgrading of bio-oils created by tail-gas reactive pyrolysis to produce pure hydrocarbons and phenols. ACS Sustain. Chem. Eng. 3, 2809–2816. https://doi.org/10.1021/acssuschemeng.5b00730.

Feng, K., Hubacek, K., Siu, Y.L., Li, X., 2014. The energy and water nexus in Chinese electricity production: a hybrid life cycle analysis. Renew. Sustain. Energy Rev. 39, 342–355. https://doi.org/10.1016/j.rser.2014.07.080.

Fernandez-Akarregi, A.R., Makibar, J., Lopez, G., Amutio, M., Olazar, M., 2013. Design and operation of a conical spouted bed reactor pilot plant (25 kg/h) for biomass fast pyrolysis. Fuel Process. Technol. 112, 48–56. https://doi.org/10.1016/j.fuproc.2013.02.022.

Fogassy, G., Thegarid, N., Toussaint, G., van Veen, A.C., Schuurman, Y., Mirodatos, C., 2010. Biomass derived feedstock co-processing with vacuum gas oil for second-generation fuel production in FCC units. Appl. Catal. B Environ. 96, 476–485. https://doi.org/10.1016/j.apcatb.2010.03.008.

Foster, A.J., Jae, J., Cheng, Y.T., Huber, G.W., Lobo, R.F., 2012. Optimizing the aromatic yield and distribution from catalytic fast pyrolysis of biomass over ZSM-5. Appl. Catal. Gen. 423–424, 154–161. https://doi.org/10.1016/j.apcata.2012.02.030.

Gan, Y., El-Houjeiri, H.M., Badahdah, A., Lu, Z., Cai, H., Przesmitzki, S., Wang, M., 2020. Carbon footprint of global natural gas supplies to China. Nat. Commun. 11, 824. https://doi.org/10.1038/s41467-020-14606-4.

Gerssen-Gondelach, S.J., Saygin, D., Wicke, B., Patel, M.K., Faaij, A.P.C., 2014. Competing uses of biomass: assessment and comparison of the performance of bio-based heat, power, fuels and materials. Renew. Sustain. Energy Rev. 40, 964–998. https://doi.org/10.1016/j.rser.2014.07.197.

Ghorbannezhad, P., Firouzabadi, M.D., Ghasemian, A., de Wild, P.J., Heeres, H.J., 2018. Sugarcane bagasse ex-situ catalytic fast pyrolysis for the production of Benzene, Toluene and Xylenes (BTX). J. Anal. Appl. Pyrolysis 131, 1–8. https://doi.org/10.1016/j.jaap.2018.02.019.

Gollakota, A.R.K., Kishore, N., Gu, S., 2018. A review on hydrothermal liquefaction of biomass. Renew. Sustain. Energy Rev. 81, 1378–1392. https://doi.org/10.1016/j.rser.2017.05.178.

Green, S.K., 2014. Production of Renewable Fuels and Chemicals from Biomass- Dervied Furan Compounds.

Gudde, N., Larivé, J., Yugo, M., 2019. Refinery 2050: Conceptual Assessment. Exploring Opportunities and Challenges for the EU Refining Industry to Transition towards a low-CO2 Intensive Economy. Concawe Special Task Force Refinery 2050 (STF-2). Brussels.

He, S., Muizebelt, I., Heeres, A., Schenk, N.J., Blees, R., Heeres, H.J., 2018. Catalytic pyrolysis of crude glycerol over shaped ZSM-5/bentonite catalysts for bio-BTX synthesis. Appl. Catal. B Environ. 235, 45–55. https://doi.org/10.1016/j.apcatb.2018.04.047.

He, S., Klein, F.G.H., Kramer, T.S., Chandel, A., Tegudeer, Z., Heeres, A., Heeres, H.J., 2021. Catalytic conversion of free fatty acids to bio-based aromatics: a model investigation using oleic acid and an H-ZSM-5/Al2O3Catalyst. ACS Sustain. Chem. Eng. 9, 1128–1141. https://doi.org/10.1021/acssuschemeng.0c06181.

Heeres, A., 2019. Catalytic Pyrolysis towards BTX Catalytic Pyrolysis towards Aromatics. Groningen.

Heeres, A., Schenk, N., Muizebelt, I., Blees, R., De Waele, B., Zeeuw, A.J., Meyer, N., Carr, R., Wilbers, E., Heeres, H.J., 2018. Synthesis of bio-aromatics from black liquors using catalytic pyrolysis. ACS Sustain. Chem. Eng. 6, 3472–3480. https://doi.org/10.1021/acssuschemeng.7b03728.

Hooey, L., Boden, A., Larsson, M., Knights, M., Johns, J., Abraham, V., Tobiesen, A., 2013. Iron and Steel CCS Study (Techno-Economics Integratedsteel Mill). IEAGHG. GLOS, UK.

Hu, Y., Tjokro Rahardjo, S., Valkenburg, C., Snowden-Swan, L., Jones, S., Machinal, M., 2011. Techno-economic Analysis for the Thermochemical Conversion of Biomass to Liquid Fuels. U.S. DOE), U.S.Department of Energy, Washington.

Huijgen, W.J.J., Smit, A.T., Reith, J.H., Uil, H. Den, 2011. Catalytic organosolv fractionation of willow wood and wheat straw as pretreatment for enzymatic cellulose hydrolysis. J. Chem. Technol. Biotechnol. 86, 1428–1438. https://doi.org/10.1002/jctb.2654.

IEA, 2017a. Energy Technology Perspectives 2017, Energy Technology Perspectives. OECD, Paris.

IEA, 2017b. Tracking Clean Energy Progress 2017:Excerpt Informing Energy Sector Transformations. IEA.

IEA, 2019a. The Future of Hydrogen- Seizing Today's Opportunities. IEA.

IEA, 2019b. Levelised Cost of CO2 Capture by Sector and Initial CO2 Concentration [WWW Document]. IEA. URL. https://www.iea.org/data-and-statistics/charts/levelised-cost-of-co2-capture-by-sector-and-initial-co2-concentration-2019, 12.6.21.

IEA, 2021. Chemicals [WWW document]. IEA. URL. https://www.iea.org/reports/chemicals, 12.5.21.

Jensen, C.U., Rodriguez Guerrero, J.K., Karatzos, S., Olofsson, G., Iversen, S.B., 2017. Fundamentals of Hydrofaction^{TM}: renewable crude oil from woody biomass. Biomass Convers. Biorefinery 7, 495–509. https://doi.org/10.1007/s13399-017-0248-8.

Ji, K., Xun, J., Liu, P., Song, Q., Gao, J., Zhang, K., Li, J., 2018. The study of methanol aromatization on transition metal modified ZSM-5 catalyst. Chin. J. Chem. Eng. 26, 1949–1953. https://doi.org/10.1016/j.cjche.2018.03.024.

Jiang, J., Feng, X., Yang, M., Wang, Y., 2020. Comparative technoeconomic analysis and life cycle assessment of aromatics production from methanol and naphtha. J. Clean. Prod. 277, 123525 https://doi.org/10.1016/j.jclepro.2020.123525.

Jones, S., Meyer, P., Snowden-Swan, L., Padmaperuma, A., Tan, E., Dutta, A., Jacobson, J., Cafferty, K., 2013. Process Design and Economics for the Conversion of Lignocellulosic Biomass to Hydrocarbon Fuels: Fast Pyrolysis and Hydrotreating Bio-Oil Pathway. Energy. https://doi.org/10.2172/1126275. Golden, CO (United States).

Kuramochi, T., Ramírez, A., Turkenburg, W., Faaij, A., 2012. Comparative assessment of CO2 capture technologies for carbon-intensive industrial processes. Prog. Energy Combust. Sci. 38, 87–112. https://doi.org/10.1016/j.pecs.2011.05.001.

Li, M.F., Chen, L.X., Li, X., Chen, C.Z., Lai, Y.C., Xiao, X., Wu, Y.Y., 2016. Evaluation of the structure and fuel properties of lignocelluloses through carbon dioxide torrefaction. Energy Convers. Manag. 119, 463–472. https://doi.org/10.1016/j.enconman.2016.04.064.

Li, X., Chalvatzis, K.J., Pappas, D., 2017a. China's electricity emission intensity in 2020 – an analysis at provincial level. Energy Proc. 142, 2779–2785. https://doi.org/10.1016/j.egypro.2017.12.421.

Li, Z., Lepore, A.W., Salazar, M.F., Foo, G.S., Davison, B.H., Wu, Z., Narula, C.K., 2017b. Selective conversion of bio-derived ethanol to renewable BTX over Ga-ZSM-5. Green Chem. 19, 4344–4352. https://doi.org/10.1039/c7gc01188a.

Lin, Z., Nikolakis, V., Ierapetritou, M., 2014. Alternative approaches for p-xylene production from starch: techno-economic analysis. Ind. Eng. Chem. Res. 53, 10688–10699. https://doi.org/10.1021/ie402469j.

Lok, C.M., Van Doorn, J., Aranda Almansa, G., 2019. Promoted ZSM-5 catalysts for the production of bio-aromatics, a review. Renew. Sustain. Energy Rev. 113, 109248 https://doi.org/10.1016/j.rser.2019.109248.

Luo, X., Liu, J., Zheng, P., Li, M., Zhou, Y., Huang, L., Chen, L., Shuai, L., 2019. Promoting enzymatic hydrolysis of lignocellulosic biomass by inexpensive soy protein. Biotechnol. Biofuels 12, 1–13. https://doi.org/10.1186/s13068-019-1387-x.

Masnadi, M.S., El-Houjeiri, H.M., Schunack, D., Li, Y., Englander, J.G., Badahdah, A., Monfort, J.-C., Anderson, J.E., Wallington, T.J., Bergerson, J.A., Gordon, D., Koomey, J., Przesmitzki, S., Azevedo, I.L., Bi, X.T., Duffy, J.E., Heath, G.A., Keoleian, G.A., McGlade, C., Meehan, D.N., Yeh, S., You, F., Wang, M., Brandt, A.R., 2018. Global carbon intensity of crude oil production, 80 Science 361, 851–853. https://doi.org/10.1126/science.aar6859.

McVey, M., Elkasabi, Y., Ciolkosz, D., 2020. Separation of BTX chemicals from biomass pyrolysis oils via continuous flash distillation. Biomass Convers. Biorefinery 10, 15–23. https://doi.org/10.1007/s13399-019-00409-1.

Meerman, J.C., Ramírez, A., Turkenburg, W.C., Faaij, A.P.C., 2012. Performance of simulated flexible integrated gasification polygeneration facilities, Part B: economic evaluation. Renew. Sustain. Energy Rev. 16, 6083–6102. https://doi.org/10.1016/j.rser.2012.06.030.

Metz, B., Davidson, O., Coninck, H. de, Loos, M., Meyer, L., 2005. Carbon Dioxide Capture and Storage. Cambridge University Press, UK.

Miandad, R., Rehan, M., Barakat, M.A., Aburiazaiza, A.S., Khan, H., Ismail, I.M.I., Dhavamani, J., Gardy, J., Hassanpour, A., Nizami, A.S., 2019. Catalytic pyrolysis of plastic waste: moving toward pyrolysis based biorefineries. Front. Energy Res. 7, 1–17. https://doi.org/10.3389/fenrg.2019.00027.

Miedema, J.H., Benders, R.M.J., Moll, H.C., Pierie, F., 2017. Renew, reduce or become more efficient? The climate contribution of biomass co-combustion in a coal-fired power plant. Appl. Energy 187, 873–885. https://doi.org/10.1016/j.apenergy.2016.11.033.

Mo, N., Pennebacker, J., Savage, P.E., 2017. Hydrocarbon chemicals from hydrothermal processing of renewable oils over HZSM-5. Biomass Convers. Biorefinery 7, 437–443. https://doi.org/10.1007/s13399-016-0231-9.

Mullen, C.A., Boateng, A.A., Goldberg, N.M., 2013. Production of deoxygenated biomass fast pyrolysis oils via product gas recycling. Energy Fuel. 27, 3867–3874. https://doi.org/10.1021/ef400739u.

Nanda, S., Vo, D.V.N., Sarangi, P.K., 2020. Biorefinery of Alternative Resources: Targeting Green Fuels and Platform Chemicals, Biorefinery of Alternative Resources: Targeting Green Fuels and Platform Chemicals. Springer Singapore, Singapore. https://doi.org/10.1007/978-981-15-1804-1.

Ng, S.H., Heshka, N.E., Zheng, Y., Wei, Q., Ding, F., 2019. FCC coprocessing oil sands heavy gas oil and canola oil. 3. Some cracking characteristics. Green Energy Environ. 4, 83–91. https://doi.org/10.1016/j.gee.2018.03.004.

OECD/IEA, 2018a. The Future of Petrochemicals-Towards More Sustainable Plastics and Fertilisers-Methodological Annex, the Future of Petrochemicals. https://doi.org/10.1787/9789264307414-en.

OECD/IEA, 2018b. The Future of Petrochemicals-Towards More Sustainable Plastics and Fertilisers.

Oliveira, C., Schure, K.M., 2020. Decarbonisation Options for the Dutch Dairy Processing Industry. PBL Netherlands Environmental Assessment Agency;TNO, The Hague.

Paysepar, H., 2018. Production of Monomeric Aromatics/phenolics from Hydrolysis Lignin (HL) by Catalytic Fast Pyrolysis and Hydrothermal Liquefaction. The University of Western Ontario.

Pinheiro Pires, A.P., Arauzo, J., Fonts, I., Domine, M.E., Fernández Arroyo, A., Garcia-Perez, M.E., Montoya, J., Chejne, F., Pfromm, P., Garcia-Perez, M., 2019. Challenges and opportunities for bio-oil refining: a review. Energy Fuel. 33, 4683–4720. https://doi.org/10.1021/acs.energyfuels.9b00039.

Pinho, A.D.R., De Almeida, M.B.B., Mendes, F.L., Ximenes, V.L., Casavechia, L.C., 2015. Co-processing raw bio-oil and gasoil in an FCC Unit. Fuel Process. Technol. 131, 159–166. https://doi.org/10.1016/j.fuproc.2014.11.008.

Pinho, A. de R., de Almeida, M.B.B., Mendes, F.L., Casavechia, L.C., Talmadge, M.S., Kinchin, C.M., Chum, H.L., 2017. Fast pyrolysis oil from pinewood chips co-processing with vacuum gas oil in an FCC unit for second generation fuel production. Fuel 188, 462–473. https://doi.org/10.1016/j.fuel.2016.10.032.

Roman-Leshkov, Y., Barrett, C.J., Liu, Z.Y., Dumesic, J.A., 2007. Production of dimethylfuran for liquid fuels from biomass-derived carbohydrates. Nature 447, 982–986. https://doi.org/10.1038/nature05923.

Ross, A.B., Biller, P., Kubacki, M.L., Li, H., Lea-Langton, A., Jones, J.M., 2010. Hydrothermal processing of microalgae using alkali and organic acids. Fuel 89, 2234–2243. https://doi.org/10.1016/j.fuel.2010.01.025.

Sami, M., Annamalai, K., Wooldridge, M., 2001. Co-firing of coal and biomass fuel blends. Prog. Energy Combust. Sci. 27, 171–214. https://doi.org/10.1016/S0360-1285(00)00020-4.

Scown, C.D., Gokhale, A.A., Willems, P.A., Horvath, A., McKone, T.E., 2014. Role of lignin in reducing life-cycle carbon emissions, water use, and cost for United States cellulosic biofuels. Environ. Sci. Technol. 48, 8446–8455. https://doi.org/10.1021/es5012753.

Sorunmu, Y.E., Billen, P., Elkasabi, Y., Mullen, C.A., Macken, N.A., Boateng, A.A., Spatari, S., 2017. Fuels and chemicals from equine-waste-derived tail gas reactive pyrolysis oil: technoeconomic analysis, environmental and exergetic life cycle assessment. ACS Sustain. Chem. Eng. 5, 8804–8814. https://doi.org/10.1021/acssuschemeng.7b01609.

Tews, I., Zhu, Y., Drennan, C.V., Elliott, D., Snowden-Swan, L.J., Onarheim, K., Solantausta, Y., Beckman, D., 2014. Biomass direct liquefaction options: technoeconomic and life cycle assessment. Pac. NW Natl. Lab. 62.

Thilakaratne, C.R., 2016. Understanding catalytic pyrolysis of biomass for production of biofuels. Iowa State University. https://doi.org/10.31274/etd-180810-5448.

TNO, 2022. Biomass source book [WWW document]. TNO. URL. https://phyllis.nl/Browse/Standard/ECN-Phyllis, 7.20.22.

Vasalos, I.A., Lappas, A.A., Kopalidou, E.P., Kalogiannis, K.G., 2016. Biomass catalytic pyrolysis: process design and economic analysis. Wiley Interdiscip. Rev. Energy Environ. 5, 370–383. https://doi.org/10.1002/wene.192.

Vispute, T.P., Zhang, H., Sanna, A., Xiao, R., Huber, G.W., 2010. Renewable chemical commodity feedstocks from integrated catalytic processing of pyrolysis oils. Science 84 330, 1222–1227. https://doi.org/10.1126/science.1194218.

Vural Gursel, I., Dijkstra, J.W., Huijgen, W.J.J., Ramirez, A., 2019. Techno-economic comparative assessment of novel lignin depolymerization routes to bio-based aromatics. Biofuels, Bioprod. Biorefining 13, 1068–1084. https://doi.org/10.1002/bbb.1999.

Wang, M., Lee, H., Molburg, J., 2004. Allocation of energy use in petroleum refineries to petroleum products. Int. J. Life Cycle Assess. 9, 34–44. https://doi.org/10.1007/BF02978534.

Wijaya, Y.P., Kristianto, I., Lee, H., Jae, J., 2016. Production of renewable toluene from biomass-derived furans via Diels-Alder and dehydration reactions: a comparative study of Lewis acid catalysts. Fuel 182, 588–596. https://doi.org/10.1016/j.fuel.2016.06.010.

Wright, M.M., Daugaard, D.E., Satrio, J.A., Brown, R.C., 2010. Techno-economic analysis of biomass fast pyrolysis to transportation fuels. Fuel 89, S2–S10. https://doi.org/10.1016/j.fuel.2010.07.029.

Yan, L., Zhang, L., Yang, B., 2014. Enhancement of total sugar and lignin yields through dissolution of poplar wood by hot water and dilute acid flowthrough pretreatment. Biotechnol. Biofuels 7. https://doi.org/10.1186/1754-6834-7-76.

Yáñez, É., Meerman, H., Ramírez, A., Castillo, É., Faaij, A., 2021. Assessing bio-oil co-processing routes as CO_2 mitigation strategies in oil refineries. Biofuels, Bioprod. Biorefining 15, 305–333. https://doi.org/10.1002/bbb.2163.

Yang, M., Shao, J., Yang, H., Chen, Y., Bai, X., Zhang, S., Chen, H., 2019a. Catalytic pyrolysis of hemicellulose for the production of light olefins and aromatics over Fe modified ZSM-5 catalysts. Cellulose 26, 8489–8500. https://doi.org/10.1007/s10570-019-02731-3.

Yang, M., Shao, J., Yang, H., Zeng, K., Wu, Z., Chen, Y., Bai, X., Chen, H., 2019b. Enhancing the production of light olefins and aromatics from catalytic fast pyrolysis of cellulose in a dual-catalyst fixed bed reactor. Bioresour. Technol. 273, 77–85. https://doi.org/10.1016/j.biortech.2018.11.005.

Yang, M., Shao, J., Yang, Z., Yang, H., Wang, X., Wu, Z., Chen, H., 2019c. Conversion of lignin into light olefins and aromatics over Fe/ZSM-5 catalytic fast pyrolysis: significance of Fe contents and temperature. J. Anal. Appl. Pyrolysis 137, 259–265. https://doi.org/10.1016/j.jaap.2018.12.003.

Yang, F., Meerman, H., Faaij, A., 2021a. Harmonized comparison of virgin steel production using biomass with carbon capture and storage for negative emissions. Int. J. Greenh. Gas Control 112, 103519. https://doi.org/10.1016/j.ijggc.2021.103519.

Yang, F., Meerman, J.C., Faaij, A.P.C., 2021b. Carbon capture and biomass in industry: a techno-economic analysis and comparison of negative emission options. Renew. Sustain. Energy Rev. 144, 111028 https://doi.org/10.1016/j.rser.2021.111028.

Zhang, B., 2021. Quantifying and Mapping Bioenergy Potentials in China: Spatiotemporal Analysis of Technical, Economic and Sustainable Biomass Supply Potentials for Optimal Biofuel Supply Chains in China. University of Groningen. https://doi.org/10.33612/diss.168012388.

Zhang, D., Jiang, J., Yang, M., Feng, X., Wang, Y., 2021a. Simulation-based superstructure optimization for the synthesis process of aromatics production from methanol. ACS Sustain. Chem. Eng. 9, 10205–10219. https://doi.org/10.1021/acssuschemeng.1c02497.

Zhang, J., Meerman, H., Benders, R., Faaij, A., 2021b. Techno-economic and life cycle greenhouse gas emissions assessment of liquefied natural gas supply chain in China. Energy 224. https://doi.org/10.1016/j.energy.2021.120049.

Zheng, A., Zhao, Z., Chang, S., Huang, Z., Wu, H., Wang, X., He, F., Li, H., 2014. Effect of crystal size of ZSM-5 on the aromatic yield and selectivity from catalytic fast pyrolysis of biomass, 383–384 J. Mol. Catal. Chem. 23–30. https://doi.org/10.1016/j.molcata.2013.11.005.

Zheng, Y., Wang, F., Yang, X., Huang, Y., Liu, C., Zheng, Z., Gu, J., 2017. Study on aromatics production via the catalytic pyrolysis vapor upgrading of biomass using metal-loaded modified H-ZSM-5. J. Anal. Appl. Pyrolysis 126, 169–179. https://doi.org/10.1016/j.jaap.2017.06.011.

Zheng, Z., Wang, J., Wei, Y., Liu, X., Yu, F., Ji, J., 2019. Effect of La-Fe/Si-MCM-41 catalysts and CaO additive on catalytic cracking of soybean oil for biofuel with low aromatics. J. Anal. Appl. Pyrolysis 143, 104693. https://doi.org/10.1016/j.jaap.2019.104693.